

CHAPTER 18

ENTANGLEMENT, ELECTRON CORRELATION, AND DENSITY MATRICES

SABRE KAIS

Department of Chemistry, Purdue University, West Lafayette, IN 47907 USA

CONTENTS

- I. Introduction
 - A. Entanglement of Formation and Concurrence
 - B. Entanglement Measure for Fermions
 - C. Entanglement and Ranks of Density Matrices
 - II. Entanglement for Spin Systems
 - A. Entanglement for Two-Spin Systems
 - B. Entanglement for One-Dimensional N -Spin Systems
 - C. Numerical Solution of the One-Dimensional Spin- $\frac{1}{2}$ Systems
 - D. Entanglement and Spin Reduced Density Matrices
 - E. Some Numerical Results
 - F. Thermal Entanglement and the Effect of Temperature
 - G. Entanglement for Two-Dimensional Spin Systems
 - III. Entanglement for Quantum Dot Systems
 - A. Two-Electron Two-Site Hubbard Model
 - 1. Exact Solution
 - 2. Hartree–Fock Approximation
 - 3. Correlation Entropy
 - 4. Entanglement
 - B. One-Dimensional Quantum Dots System
 - C. Two-Dimensional Array of Quantum Dots
 - IV. Ab Initio Calculations and Entanglement
 - V. Dynamics of Entanglement and Decoherence
 - VI. Entanglement and Density Functional Theory
 - VII. Future Directions
- Acknowledgments
References

Reduced-Density-Matrix Mechanics: With Application to Many-Electron Atoms and Molecules, A Special Volume of Advances in Chemical Physics, Volume 134, edited by David A. Mazziotti. Series editor Stuart A. Rice. Copyright © 2007 John Wiley & Sons, Inc.

I. INTRODUCTION

In quantum chemistry calculations, the correlation energy is defined as the energy error of the Hartree–Fock wavefunction, that is, the difference between the Hartree–Fock limit energy and the exact solution of the nonrelativistic Schrödinger equation [1]. Different types of electron correlation are often distinguished in quantum chemistry such as dynamical and nondynamical [2], radial versus angular correlation for atoms, left–right, in–out and, radial correlation for diatomic molecules, and weak and strong correlation for solids. There also exists other measures of electron correlation in the literature such as the statistical correlation coefficients [3] and more recently the Shannon entropy as a measure of the correlation strength [4–8]. Correlation of a quantum many-body state makes the one-particle density matrix nonidempotent. Therefore the Shannon entropy of the natural occupation numbers measures the correlation strength on the one-particle level [7]. Electron correlations have a strong influence on many atomic, molecular [9], and solid properties [10]. The concept of electron correlation as defined in quantum chemistry calculations is useful but not directly observable; that is, there is no operator in quantum mechanics that its measurement gives the correlation energy. Moreover, there are cases where the kinetic energy dominates the Coulomb repulsion between electrons, so the electron correlation alone fails as a correlation measure [6].

Entanglement is a quantum mechanical property that describes a correlation between quantum mechanical systems and has no classical analogue [11–15]. Schrödinger was the first to introduce these states and gave them the name “Verschränkung” to a correlation of quantum nature [16]: “For an entangled state the best possible knowledge of the whole does not include the best possible knowledge of its parts.” Latter, Bell [17] defined entanglement as “a correlation that is stronger than any classical correlation.” Thus it might be useful as an alternative measure of electron–electron correlation in quantum chemistry calculations.

Ever since the appearance of the famous EPR Gedanken experiment [18], the phenomenon of entanglement [19], which features the essential difference between classical and quantum physics, has received wide theoretical and experimental attention [17, 20–25]. Generally, if two particles are in an entangled state then, even if the particles are physically separated by a great distance, they behave in some respects as a single entity rather than as two separate entities. There is no doubt that the entanglement has been lying in the heart of the foundation of quantum mechanics.

A desire to understand quantum entanglement is fueled by the development of quantum computation, which started in the 1980s with the pioneering work of Benioff [26], Bennett [27], Deutsch [28], Feynman [29] and Landauer [30] but gathered momentum and research interest only after Peter Shor’s revolutionary

discovery [31] of a quantum computer algorithm in 1994 that would efficiently find the prime factors of composite integers. Since integer factorization is the basis for cryptosystems used for security nowadays, Shor's finding will have a profound effect on cryptography. The astronomical power of quantum computations has researchers all over the world racing to be the first to create a practical quantum computer.

Besides quantum computations, entanglement has also been at the core of other active research such as quantum teleportation [32, 33], dense coding [34, 35], quantum communication [36], and quantum cryptography [37]. It is believed that the conceptual puzzles posed by entanglement have now become a physical source of novel ideas that might result in applications.

A big challenge faced by all of the above-mentioned applications is to prepare the entangled states, which is much more subtle than classically correlated states. To prepare an entangled state of good quality is a preliminary condition for any successful experiment. In fact, this is not only an experimental problem but also poses an obstacle to theories, since how to quantify entanglement is still unsettled; this is now becoming one of the central topics in quantum information theory. Any function that quantifies entanglement is called an entanglement measure. It should tell us how much entanglement there is in a given multipartite state. Unfortunately, there is currently no consensus as to the best method to define an entanglement for all possible multipartite states. And the theory of entanglement is only partially developed [13, 38–40] and for the moment can only be applied in a limited number of scenarios, where there is an unambiguous way to construct suitable measures. Two important scenarios are (i) the case of a pure state of a bipartite system, that is, a system consisting of only two components and (ii) a mixed state of two spin- $\frac{1}{2}$ particles.

When a bipartite quantum system AB describe by $H_A \otimes H_B$ is in a pure state, there is an essentially well-motivated and unique measure of the entanglement between the subsystems A and B given by the von Neumann entropy S . If we denote with ρ_A the partial trace of $\rho \in H_A \otimes H_B$ with respect to subsystem B, $\rho_A = \text{Tr}_B(\rho)$, the entropy of entanglement of the state ρ is defined as the von Neumann entropy of the reduced density operator ρ_A , $S(\rho) \equiv -\text{Tr}[\rho_A \log_2 \rho_A]$. It is possible to prove that, for the pure state, the quantity S does not change if we exchange A and B. So we have $S(\rho) \equiv -\text{Tr}[\rho_A \log_2 \rho_A] \equiv -\text{Tr}[\rho_B \log_2 \rho_B]$. For any bipartite pure state, if an entanglement $E(\rho)$ is said to be a good one, it is often required to have the following properties [14]:

- *Separability*: If ρ is separable, then $E(\rho) = 0$.
- *Normalization*: The entanglement of a maximally entangled state of two d -dimensional systems is given by $E = \log(d)$.

- *No Increase Under Local Operations*: Applying local operations and classically communicating cannot increase the entanglement of ρ .
- *Continuity*: In the limit of vanishing distance between two density matrices, the difference between their entanglement should tend to zero.
- *Additivity*: A certain number N of identical copies of the state ρ should contain N times the entanglement of one copy.
- *Subadditivity*: The entanglement of the tensor product of two states should not be larger than the sum of the entanglement of each of the states.
- *Convexity*: The entanglement measure should be a convex function, that is, $E(\lambda\rho + (1 - \lambda)\sigma) \leq \lambda E(\rho) + (1 - \lambda)E(\sigma)$ for $0 < \lambda < 1$.

For a pure bipartite state, it is possible to show that the von Neumann entropy of its reduced density matrix, $S(\rho_{\text{red}}) = -\text{Tr}(\rho_{\text{red}} \log_2 \rho_{\text{red}})$, has all the above properties. Clearly, S is not the only mathematical object that meets the requirement, but in fact, it is now basically accepted as the correct and unique measure of entanglement.

The strict definitions of the four most prominent entanglement measures can be summarized as follows [14]:

- *Entanglement of distillation* E_D .
- *Entanglement of cost* E_C .
- *Entanglement of formation* E_F .
- *Relative entropy of entanglement* E_R .

The first two measures are also called operational measures, while the second two don't admit a direct operational interpretation in terms of entanglement manipulations. Suppose E is a measure defined on mixed states that satisfy the conditions for a good measure mentioned above. Then we can prove that for all states $\rho \in (H^A \otimes H^B)$, $E_D(\rho) \leq E(\rho) \leq E_C(\rho)$, and both $E_D(\rho)$ and $E_C(\rho)$ coincide on pure states with the von Neumann reduced entropy as demonstrated earlier.

A. Entanglement of Formation and Concurrence

At the current time, there is no simple way to carry out the calculations with all these entanglement measures. Their properties, such as additivity, convexity, and continuity, and relationships are still under active investigation. Even for the best-understood entanglement of formation of the mixed states in bipartite systems AB, once the dimension of A or B is three or above, we don't know how to express it simply, although we have the general definitions given previously. However, for the case where both subsystems A and B are spin- $\frac{1}{2}$ particles, there exists a simple formula from which the entanglement of formation can be calculated [42].

Given a density matrix ρ of a pair of quantum systems A and B and all possible pure-state decompositions of ρ

$$\rho = \sum_i p_i |\psi_i\rangle\langle\psi_i| \quad (1)$$

where p_i are the probabilities for ensembles of states $|\psi_i\rangle$, the entanglement E is defined as the entropy of either of the subsystems A or B:

$$E(\psi) = -\text{Tr}(\rho_A \log_2 \rho_A) = -\text{Tr}(\rho_B \log_2 \rho_B) \quad (2)$$

The entanglement of formation of the mixed ρ is then defined as the average entanglement of the pure states of the decomposition [42], minimized over all decompositions of ρ :

$$E(\rho) = \min \sum_i p_i E(\psi_i) \quad (3)$$

For a pair of qubits this equation can be written [42–44]

$$E(\rho) = \varepsilon(C(\rho)) \quad (4)$$

where ε is a function of the “concurrence” C :

$$\varepsilon(C) = h\left(\frac{1 + \sqrt{1 - C^2}}{2}\right) \quad (5)$$

where h is the binary entropy function [20]

$$h(x) = -x \log_2 x - (1 - x) \log_2 (1 - x) \quad (5)$$

In this case the entanglement of formation is given in terms of another entanglement measure, the concurrence C [42–44]. The entanglement of formation varies monotonically with the concurrence. From the density matrix of the two-spin mixed states, the concurrence can be calculated as follows:

$$C(\rho) = \max[0, \lambda_1 - \lambda_2 - \lambda_3 - \lambda_4] \quad (6)$$

where λ_i are the eigenvalues in decreasing order of the Hermitian matrix $R \equiv \sqrt{\sqrt{\rho} \tilde{\rho} \sqrt{\rho}}$ with $\tilde{\rho} = (\sigma^y \otimes \sigma^y) \rho^* (\sigma^y \otimes \sigma^y)$. Here σ^y is the Pauli matrix of

the spin in the y direction. The concurrence varies from $C = 0$ for a separable state to $C = 1$ for a maximally entangled state. The concurrence as a measure of entanglement will be used in Section II to discuss tuning and manipulating the entanglement for spin systems.

B. Entanglement Measure for Fermions

As we discussed in the previous section, for distinguishable particles, the most suitable and famous measure of entanglement is Wootters' measure [42], the entanglement of formation or concurrence. Recently, Schlieman and co-workers [45, 46] examined the influence of quantum statistics on the definition of entanglement. They discussed a two-fermion system with the Slater decomposition instead of Schmidt decomposition for the entanglement measure. If we take each of the indistinguishable fermions to be in the single-particle Hilbert space C^N , with f_m, f_m^+ ($m = 1, \dots, N$) denoting the fermionic annihilation and creation operators of single-particle states and $|\Omega\rangle$ representing the vacuum state, then a pure two-electron state can be written

$$\sum_{m,n} \omega_{mn} f_m^+ f_n^+ |\Omega\rangle,$$

where $\omega_{mn} = -\omega_{nm}$.

Analogous to the Schmidt decomposition, it can be proved that every $|\Psi\rangle$ can be represented in an appropriately chosen basis in C^N in a form of Slater decomposition [45],

$$|\Psi\rangle = \frac{1}{\sqrt{\sum_{i=1}^K |z_i|^2}} \sum_{i=1}^K z_i f_{a_1(i)}^+ f_{a_2(i)}^+ |\Omega\rangle \quad (7)$$

where $f_{a_1(i)}^+ |\Omega\rangle, f_{a_2(i)}^+ |\Omega\rangle$, $i = 1, \dots, K$, form an orthonormal basis in C^N . The number of nonvanishing coefficients z_i is called the Slater rank, which is then used for the entanglement measure. With similar technique, the case of a two-boson system is studied by Li et al. [47] and Paškauskas and you [48].

Gittings and Fisher [49] put forward three desirable properties of any entanglement measure: (i) invariance under local unitary transformations; (ii) noninvariance under nonlocal unitary transformations; and (iii) correct behavior as distinguishability of the subsystems is lost. These requirements make the relevant distinction between one-particle unitary transformation and one-site unitary transformations. A natural way to achieve this distinction [49] is to use a basis based on sites rather than on particles. Through the Gittings–Fisher investigation, it is shown that all of the above-discussed entanglement measures fail the tests of the three criteria. Only Zanardi's

measure [50] survives, which is given in Fock space as the von Neumann entropy, namely,

$$E_j = -\text{Tr} \rho_j \log_2 \rho_j, \quad \rho_j = \text{Tr}_j |\psi\rangle\langle\psi| \quad (8)$$

where Tr_j denotes the trace over all but the j th site and ψ is the antisymmetric wavefunction of the studied system. Hence E_j actually describes the entanglement of the j th site with the remaining sites. A generalization of this one-site entanglement is to define an entanglement between one L -site block with the rest of the system [51],

$$E_L = -\text{Tr}(\rho_L \log_2 \rho_L) \quad (9)$$

C. Entanglement and Ranks of Density Matrices

In this section we review the known theorems that relate entanglement to the ranks of density matrices [52]. The rank of a matrix ρ , denoted as $\text{rank}(\rho)$, is the maximal number of linearly independent row vectors (also column vectors) in the matrix ρ . Based on the ranks of reduced density matrices, one can derive necessary conditions for the separability of multiparticle arbitrary-dimensional mixed states, which are equivalent to sufficient conditions for entanglement [53]. For convenience, let us introduce the following definitions [54–56]. A pure state ρ of N particles A_1, A_2, \dots, A_N is called entangled when it cannot be written

$$\rho = \rho_{A_1} \otimes \rho_{A_2} \otimes \dots \otimes \rho_{A_N} = \bigotimes_{i=1}^N \rho_{A_i} \quad (10)$$

where ρ_{A_i} is the single-particle reduced density matrix given by $\rho_{A_i} \equiv \text{Tr}_{\{A_j\}}(\rho)$ for $\{A_j | \text{all } A_j \neq A_i\}$. A mixed state ρ of N particles A_1, A_2, \dots, A_N , described by M probabilities p_j and M pure states ρ^j as $\rho = \sum_{j=1}^M p_j \rho^j$, is called entangled when it cannot be written

$$\rho = \sum_{j=1}^M p_j \bigotimes_{i=1}^N \rho_{A_i}^j \quad (11)$$

where $p_j > 0$ for $j = 1, 2, \dots, M$ with $\sum_{j=1}^M p_j = 1$.

Now we are in a position to list the separability conditions without proof. (The reader who is interested in the formal proofs can consult the paper by Chong, Keiter, and Stolze [53].)

Lemma 1 *A state is pure if and only if the rank of its density matrix ρ is equal to 1, that is, $\text{rank}(\rho) = 1$.*

Lemma 2 *A pure state is entangled if and only if the rank of at least one of its reduced density matrices is greater than 1.*

Lemma 3 *Given a pure state ρ , if its particles are separated into two parts U and V , then $\text{rank}(\rho_U) = 1$ holds if and only if these two parts are separable, that is, $\rho = \rho_U \otimes \rho_V$.*

Now we can discuss the necessary conditions for separable states. For convenience, we will use the following notation. For a state ρ of N particles A_1, A_2, \dots, A_N , the reduced density matrix obtained by tracing ρ over particle A_i is written $\rho_{R(i)} = \text{Tr}_{A_i}(\rho)$, where $R(i)$ denotes the set of the remaining $(N-1)$ particles other than particle A_i . In the same way, $\rho_{R(i,j)} = \text{Tr}_{A_j}(\rho_{R(i)}) = \text{Tr}_{A_j}(\text{Tr}_{A_i}(\rho)) = \text{Tr}_{A_i}(\text{Tr}_{A_j}(\rho))$ denotes the reduced density matrix obtained by tracing ρ over particles A_i and A_j , $\rho_{R(i,j,k)} = \text{Tr}_{A_k}(\text{Tr}_{A_j}(\text{Tr}_{A_i}(\rho)))$, and so on. In view of these relations, ρ can be called the 1-level-higher density matrix of $\rho_{R(i)}$ and 2-level-higher density matrix of $\rho_{R(i,j)}$; $\rho_{R(i)}$ can be called the 1-level-higher density matrix of $\rho_{R(i,j)}$ and 2-level-higher density matrix of $\rho_{R(i,j,k)}$; and so on.

Now let us define the *separability condition theorem* [53]. If a state ρ of N particles A_1, A_2, \dots, A_N is separable, then the rank of any reduced density matrix of ρ must be less than or equal to the ranks of all of its 1-level-higher density matrices; that is,

$$\text{rank}(\rho_{R(i)}) \leq \text{rank}(\rho) \quad (12)$$

holds for any $A_i \in \{A_1, A_2, \dots, A_N\}$; and

$$\text{rank}(\rho_{R(i,j)}) \leq \text{rank}(\rho_{R(i)}), \quad \text{rank}(\rho_{R(i,j)}) \leq \text{rank}(\rho_{R(j)}) \quad (13)$$

holds for any pair of all particles.

This will lead to the conditions for a mixed state to be entangled. *Given a mixed state ρ , if the rank of at least one of the reduced density matrices of ρ is greater than the rank of one of its 1-level-higher density matrices, then the state ρ is entangled.*

II. ENTANGLEMENT FOR SPIN SYSTEMS

A. Entanglement for Two-Spin Systems

We consider a set of N localized spin- $\frac{1}{2}$ particles coupled through exchange interaction J and subject to an external magnetic field of strength B . In this section we

will demonstrate that (i) entanglement can be controlled and tuned by varying the anisotropy parameter in the Hamiltonian and by introducing impurities into the systems; (ii) for certain parameters, the entanglement is zero up to a critical point λ_c , where a quantum phase transition occurs, and is different from zero above λ_c ; and (iii) entanglement shows scaling behavior in the vicinity of the transition point.

For simplicity, let us illustrate the calculations of entanglement for two spin- $\frac{1}{2}$ particles. The general Hamiltonian, in atomic units, for such a system is given by [57]

$$H = -\frac{J}{2}(1 + \gamma)\sigma_1^x \otimes \sigma_2^x - \frac{J}{2}(1 - \gamma)\sigma_1^y \otimes \sigma_2^y - B\sigma_1^z \otimes I_2 - BI_1 \otimes \sigma_2^z \quad (14)$$

where σ^a are the Pauli matrices ($a = x, y, z$) and γ is the degree of anisotropy. For $\gamma = 1$ Eq. (14) reduces to the Ising model, whereas for $\gamma = 0$ it is the XY model.

This model admits an exact solution; it is simply a (4×4) matrix of the form

$$H = \begin{pmatrix} -2B & 0 & 0 & -J\gamma \\ 0 & 0 & -J & 0 \\ 0 & -J & 0 & 0 \\ -J\gamma & 0 & 0 & 2B \end{pmatrix} \quad (15)$$

with the following four eigenvalues,

$$\lambda_1 = -J, \quad \lambda_2 = J, \quad \lambda_3 = -\sqrt{4B^2 + J^2\gamma^2}, \quad \lambda_4 = \sqrt{4B^2 + J^2\gamma^2} \quad (16)$$

and the corresponding eigenvectors,

$$|\phi_1\rangle = \begin{pmatrix} 0 \\ 1/\sqrt{2} \\ 1/\sqrt{2} \\ 0 \end{pmatrix}, \quad |\phi_2\rangle = \begin{pmatrix} 0 \\ -1/\sqrt{2} \\ 1/\sqrt{2} \\ 0 \end{pmatrix} \quad (17)$$

$$|\phi_3\rangle = \begin{pmatrix} \sqrt{\frac{\alpha + 2B}{2\alpha}} \\ 0 \\ 0 \\ \sqrt{\frac{\alpha - 2B}{2\alpha}} \end{pmatrix}, \quad |\phi_4\rangle = \begin{pmatrix} -\sqrt{\frac{\alpha - 2B}{2\alpha}} \\ 0 \\ 0 \\ \sqrt{\frac{\alpha + 2B}{2\alpha}} \end{pmatrix} \quad (18)$$

where $\alpha = \sqrt{4B^2 + J^2\gamma^2}$. In the basis set $\{|\uparrow\uparrow\rangle, |\uparrow\downarrow\rangle, |\downarrow\uparrow\rangle, |\downarrow\downarrow\rangle\}$, the eigenvectors can be written

$$|\phi_1\rangle = \frac{1}{\sqrt{2}}(|\downarrow\uparrow\rangle + |\uparrow\downarrow\rangle) \quad (19)$$

$$|\phi_2\rangle = \frac{1}{\sqrt{2}}(|\downarrow\uparrow\rangle - |\uparrow\downarrow\rangle) \quad (20)$$

$$|\phi_3\rangle = \sqrt{\frac{\alpha - 2B}{2\alpha}}|\downarrow\downarrow\rangle + \sqrt{\frac{\alpha + 2B}{2\alpha}}|\uparrow\uparrow\rangle \quad (21)$$

$$|\phi_4\rangle = \sqrt{\frac{\alpha + 2B}{2\alpha}}|\downarrow\downarrow\rangle - \sqrt{\frac{\alpha - 2B}{2\alpha}}|\uparrow\uparrow\rangle \quad (22)$$

Now we confine our interest to the calculation of entanglement between the two spins. For simplicity, we take $\gamma = 1$; Eq. (14) reduces to the Ising model with the ground-state energy λ_3 and the corresponding eigenvector $|\phi_3\rangle$. All the information needed for quantifying the entanglement in this case is contained in the reduced density matrix $\rho(i, j)$ [42–44].

For our model system in the ground state $|\phi_3\rangle$, the density matrix in the basis set $(\uparrow\uparrow, \uparrow\downarrow, \downarrow\uparrow, \downarrow\downarrow)$ is given by

$$\rho = \begin{pmatrix} \frac{\alpha + 2B}{2\alpha} & 0 & 0 & \sqrt{\frac{\alpha^2 - 4B^2}{4\alpha^2}} \\ 0 & 0 & 0 & 0 \\ 0 & 0 & 0 & 0 \\ \sqrt{\frac{\alpha^2 - 4B^2}{4\alpha^2}} & 0 & 0 & \frac{\alpha + 2B}{2\alpha} \end{pmatrix} \quad (23)$$

The eigenvalues of the Hermitian matrix R needed to calculate the concurrence [42], C , Eq. (6), can be calculated analytically. We obtained $\lambda_2 = \lambda_3 = \lambda_4 = 0$ and therefore

$$C(\rho) = \lambda_1 = \sqrt{\frac{\lambda^2}{4 + \lambda^2}} \quad (24)$$

where $\lambda = J/B$. Entanglement is a monotonically increasing function of the concurrence and is given by

$$E(C) = h(y) = -y \log_2 y - (1 - y) \log_2 (1 - y); \quad y = \frac{1}{2} + \frac{1}{2} \sqrt{1 - C^2} \quad (25)$$

Substituting the value of the concurrence C , Eq. (24) gives

$$E = -\frac{1}{2} \log_2 \left(\frac{1}{4} - \frac{1}{4 + \lambda^2} \right) + \frac{1}{\sqrt{4 + \lambda^2}} \log_2 \frac{\sqrt{4 + \lambda^2} - 2}{\sqrt{4 + \lambda^2} + 2} \quad (26)$$

This result for entanglement is equivalent to the von Neumann entropy of the reduced density matrix ρ_A . For our model system of the form AB in the ground state $|\phi_3\rangle$, the reduced density matrix $\rho_A = \text{Tr}_B(\rho_{AB})$ in the basis set (\uparrow, \downarrow) is given by

$$\rho_A = \begin{pmatrix} \frac{\alpha + 2B}{2\alpha} & 0 \\ 0 & \frac{\alpha - 2B}{2\alpha} \end{pmatrix} \quad (27)$$

As we mentioned before, when a biparticle quantum system AB is in a pure state, there is essentially a unique measure of the entanglement between the subsystems A and B given by the von Neumann entropy $S \equiv -\text{Tr}[\rho_A \log_2 \rho_A]$. This approach gives exactly the same formula as the one given in Eq. (26). This is not surprising since all entanglement measures should coincide on pure bipartite states and be equal to the von Neumann entropy of the reduced density matrix (uniqueness theorem).

This simple model can be used to examine the entanglement for two-electron diatomic molecules. The value of J , the exchange coupling constant between the spins of the two electrons, can be calculated as half the energy difference between the lowest singlet and triplet states of the hydrogen molecule. Herring and Flicker [58] have shown that J for the H_2 molecule can be approximated as a function of the interatomic distance R . In atomic units, the expression for large R is given by

$$J(R) = -0.821 R^{5/2} e^{-2R} + O(R^2 e^{-2R}) \quad (28)$$

Figure 1 shows the calculated concurrence $C(\rho)$ as a function of the distance between the two electronic spins R , using $J(R)$ of Eq. (28), for different values of the magnetic field strength B . At the limit $R \rightarrow \infty$ the exchange interaction J vanishes as a result of the two electronic spins being up and the wavefunction being factorizable; that is, the concurrence is zero. At the other limit, when $R = 0$ the concurrence or the entanglement is zero for this model because $J = 0$. As R increases, the exchange interaction increases, leading to increasing concurrence between the two electronic spins. However, this increase in the concurrence reaches a maximum limit as shown in the figure. For large distance, the exchange interaction decreases exponentially with R and thus the decrease of the concurrence. Figure 1 also shows that the concurrence increases with decreasing magnetic field strength. This can be attributed to effectively increasing the exchange interaction. This behavior of the concurrence as a function of the internuclear distance R is typical for two-electron diatomic molecules. We will show later in Section IV that by using accurate ab initio calculations we essentially obtain qualitatively the same curve for entanglement for the H_2 molecule as a function of the internuclear distance R .

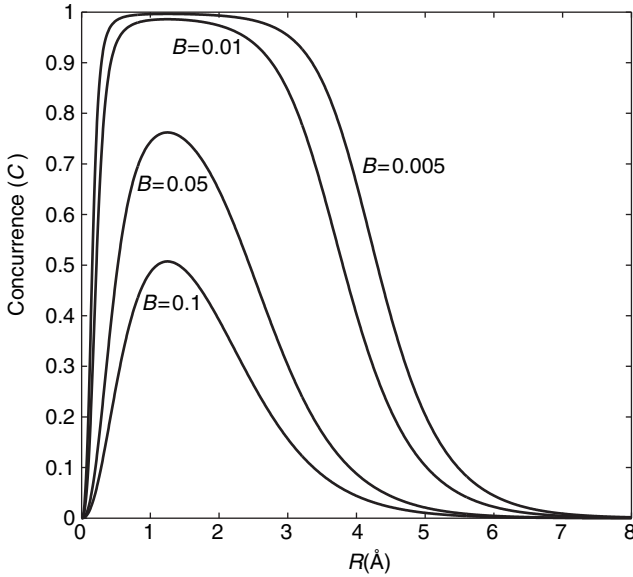


Figure 1. The concurrence (C) as a function of the distance R between the two spins for different values of the magnetic field strength B .

B. Entanglement for One-Dimensional N -Spin Systems

Now let us generalize it to a one-dimensional lattice with N sites in a transverse magnetic field and with impurities. The Hamiltonian for such a system is given by [59]

$$H = -\frac{1+\gamma}{2} \sum_{i=1}^N J_{i,i+1} \sigma_i^x \sigma_{i+1}^x - \frac{1-\gamma}{2} \sum_{i=1}^N J_{i,i+1} \sigma_i^y \sigma_{i+1}^y - \sum_{i=1}^N B_i \sigma_i^z \quad (29)$$

where $J_{i,i+1}$ is the exchange interaction between sites i and $i+1$, B_i is the strength of the external magnetic field at site i , σ^a are the Pauli matrices ($a = x, y, z$), γ is the degree of anisotropy, and N is the number of sites. We assume cyclic boundary conditions, so that

$$\sigma_{N+1}^x = \sigma_1^x, \quad \sigma_{N+1}^y = \sigma_1^y, \quad \sigma_{N+1}^z = \sigma_1^z \quad (30)$$

For $\gamma = 1$ the Hamiltonian reduces to the Ising model and for $\gamma = 0$ to the XY model. For the pure homogeneous case, $J_{i,i+1} = J$ and $B_i = B$, the system exhibits a quantum phase transition at a dimensionless coupling constant

$\lambda = J/2B = 1$. The magnetization $\langle \sigma^x \rangle$ is different from zero for $\lambda > 1$ and it vanishes at the transition point. The magnetization along the z direction $\langle \sigma^z \rangle$ is different from zero for any value of λ . At the phase transition point, the correlation length ξ diverges as $\xi \sim |\lambda - \lambda_c|^{-\nu}$ with $\nu = 1$ [60].

C. Numerical Solution of the One-Dimensional Spin- $\frac{1}{2}$ Systems

The standard procedure used to solve Eq. (29) is to transform the spin operators into fermionic operators [61]. Let us define the raising and lowering operators a_i^+ , a_i^- :

$$a_i^+ = \frac{1}{2}(\sigma_i^x + i\sigma_i^y); \quad a_i^- = \frac{1}{2}(\sigma_i^x - i\sigma_i^y)$$

Then we introduce the Fermi operators c_i, c_i^+ defined by

$$a_i^- = \exp\left(-\pi i \sum_{j=1}^{i-1} c_j^+ c_j\right) c_i; \quad a_i^+ = c_i^+ \exp\left(\pi i \sum_{j=1}^{i-1} c_j^+ c_j\right)$$

So the Hamiltonian assumes the following quadratic form:

$$H = - \sum_{i=1}^N J_{i,i+1} [(c_i^+ c_{i+1} + \gamma c_i^+ c_{i+1}^+) + \text{h.c.}] - 2 \sum_{i=1}^N B_i (c_i^+ c_i - \frac{1}{2}) \quad (31)$$

$$\lambda = J/2B$$

We can write the parameters $J_{i,i+1} = J(1 + \alpha_{i,i+1})$, where α introduces the impurity in the exchange interactions, and the external magnetic field takes the form $B_i = B(1 + \beta_i)$, where β measures the impurity in the magnetic field. When $\alpha = \beta = 0$ we recover the pure XY case.

Introducing the matrices \mathbf{A} , \mathbf{B} , where \mathbf{A} is symmetrical and \mathbf{B} is antisymmetrical, we can rewrite the Hamiltonian:

$$H' = \sum_{i,j=1}^N \left[c_i^+ A_{ij} c_j + \frac{1}{2} (c_i^+ B_{i,j} c_j^+ + \text{h.c.}) \right]$$

Introducing linear transformation, we have

$$\eta_k = \sum_{i=1}^N g_{ki} c_i + h_{ki} c_i^+; \quad \eta_k^+ = \sum_{i=1}^N g_{ki} c_i^+ + h_{ki} c_i$$

with the g_{ki} and h_{ki} real and which will give the Hamiltonian form

$$H = \sum_k^N \Lambda_k \eta_k^\dagger \eta_k + \text{constant}$$

From these conditions, we can get a set of equations for the g_{ki} and h_{ki} :

$$\Lambda_k g_{ki} = \sum_{j=1}^N (g_{kj} \mathbf{A}_{ji} - h_{kj} \mathbf{B}_{ji}) \quad (32)$$

$$\Lambda_k h_{ki} = \sum_{j=1}^N (g_{kj} \mathbf{B}_{ji} - h_{kj} \mathbf{A}_{ji}) \quad (33)$$

By introducing the linear combinations

$$\phi_{ki} = g_{ki} + h_{ki}; \quad \psi_{ki} = g_{ki} - h_{ki}$$

we can get the coupled equation

$$\phi_k (A - B) = \Lambda_k \psi_k \quad \text{and} \quad \psi_k (A + B) = \Lambda_k \phi_k$$

Then we can get both ϕ_k and ψ_k vectors from these two equations by the numerical method [62]. The ground state of the system corresponds to the state of “no-particles” and is denoted as $|\Psi_0\rangle$, and

$$\eta_k |\Psi_0\rangle = 0, \quad \text{for all } k$$

D. Entanglement and Spin Reduced Density Matrices

The matrix elements of the reduced density matrix needed to calculate the entanglement can be written in terms of the spin–spin correlation functions and the average magnetization per spin. The spin–spin correlation functions for the ground state are defined as [62]

$$S_{lm}^x = \frac{1}{4} \langle \Psi_0 | \sigma_l^x \sigma_m^x | \Psi_0 \rangle$$

$$S_{lm}^y = \frac{1}{4} \langle \Psi_0 | \sigma_l^y \sigma_m^y | \Psi_0 \rangle$$

$$S_{lm}^z = \frac{1}{4} \langle \Psi_0 | \sigma_l^z \sigma_m^z | \Psi_0 \rangle$$

and the average magnetization per spin is

$$M_i^z = \frac{1}{2} \langle \Psi_0 | \sigma_i^z | \Psi_0 \rangle \quad (34)$$

These correlation functions can be obtained using the set ψ_k and ϕ_k from the previous section.

The structure of the reduced density matrix follows from the symmetry properties of the Hamiltonian. However, for this case the concurrence $C(i, j)$ depends on i, j and the location of the impurity and not only on the difference $|i - j|$ as for the pure case. Using the operator expansion for the density matrix and the symmetries of the Hamiltonian leads to the general form

$$\rho = \begin{pmatrix} \rho_{1,1} & 0 & 0 & \rho_{1,4} \\ 0 & \rho_{2,2} & \rho_{2,3} & 0 \\ 0 & \rho_{2,3} & \rho_{3,3} & 0 \\ \rho_{1,4} & 0 & 0 & \rho_{4,4} \end{pmatrix} \quad (35)$$

with

$$\lambda_a = \sqrt{\rho_{1,1}\rho_{4,4} + |\rho_{1,4}|}, \quad \lambda_b = \sqrt{\rho_{2,2}\rho_{3,3} + |\rho_{2,3}|} \quad (36)$$

$$\lambda_c = |\sqrt{\rho_{1,1}\rho_{4,4}} - |\rho_{1,4}||, \quad \lambda_d = |\sqrt{\rho_{2,2}\rho_{3,3}} - |\rho_{2,3}|| \quad (37)$$

Using the definition $\langle A \rangle = \text{Tr}(\rho A)$, we can express all the matrix elements in the density matrix in terms of different spin-spin correlation functions [62]:

$$\rho_{1,1} = \frac{1}{2}M_l^z + \frac{1}{2}M_m^z + S_{lm}^z + \frac{1}{2} \quad (38)$$

$$\rho_{2,2} = \frac{1}{2}M_l^z - \frac{1}{2}M_m^z - S_{lm}^z + \frac{1}{4} \quad (39)$$

$$\rho_{3,3} = \frac{1}{2}M_m^z - \frac{1}{2}M_l^z - S_{lm}^z + \frac{1}{4} \quad (40)$$

$$\rho_{4,4} = -\frac{1}{2}M_l^z - \frac{1}{2}M_m^z + S_{lm}^z + \frac{1}{4} \quad (41)$$

$$\rho_{2,3} = S_{lm}^x + S_{lm}^y \quad (42)$$

$$\rho_{1,4} = S_{lm}^x - S_{lm}^y \quad (43)$$

E. Some Numerical Results

Let us show how the entanglement can be tuned by changing the anisotropy parameter γ by going from the Ising model ($\gamma = 1$) to the XY model ($\gamma = 0$). For the XY model the entanglement is zero up to the critical point λ_c and is different from zero above λ_c . Moreover, by introducing impurities, the entanglement can be tuned down as the strength of the impurity α increases [59]. First, we examine the change of the entanglement for the Ising model ($\gamma = 1$) for different values of the impurity strength α as the parameter λ , which induces the quantum phase transitions, varies. Figure 2 shows the change of the nearest-neighbor concurrence $C(1, 2)$ with the impurity located at $i_m = 3$ as a

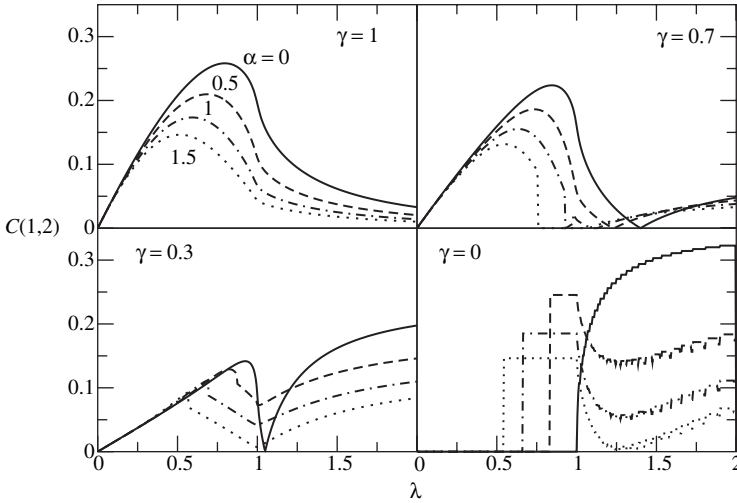


Figure 2. The nearest-neighbor concurrence $C(1,2)$ for different values of the anisotropy parameter $\gamma = 1, 0.7, 0.3, 0$ with an impurity located at $i_m = 3$ as a function of the reduced coupling constant $\lambda = J/2h$, where J is the exchange interaction constant and h is the strength of the external magnetic field. The curves correspond to different values of the impurity strength $\alpha = 0, 0.5, 1, 1.5$ with system size $N = 201$.

function of λ for different values of α . One can see clearly in Figure 2 that the entanglement can be tuned down by increasing the value of the parameter α . For $\alpha = 1.5$, the concurrence approaches zero above the critical $\lambda_c = 1$. The system size was taken as $N = 201$ based on finite size scaling analysis. Analysis of all the results for the pure case ($\alpha = 0$) for different system sizes ranging from $N = 41$ up to $N = 401$ collapse into a single curve. Thus all key ingredients of the finite size scaling are present in the concurrence. This holds true for the impurity problem as long as we consider the behavior of the value of λ for which the derivative of the concurrence attains its minimum value versus the system size. As expected, there is no divergence of the derivative $dC(1, 2)/d\lambda$ for finite N , but there are clear anomalies. By examining $\ln(\lambda_c - \lambda_m)$ versus $\ln N$ for $\alpha = 0.1$, one obtains that the minimum λ_m scales as $\lambda_m \sim \lambda_c + N^{-0.93}$ and $dC(1, 2)/d\lambda$ diverges logarithmically with increasing system size. For a system with the impurity located at larger distance $i_m = 10$ and the same $\alpha = 0.1$, $\lambda_m \sim \lambda_c + N^{-0.85}$, showing that the scaling behavior depends on the distance between the impurity and the pair of sites under consideration.

Figure 2 also shows the variation of nearest-neighbor concurrence as the anisotropy parameter γ decreases. For the XY model ($\gamma = 0$), the concurrence for $\alpha = 0$ is zero up to the critical point $\lambda_c = 1$ and different from zero above $\lambda_c = 1$. However, as α increases the concurrence develops steps and the

results strongly depend on the system size. For small system size, such as $N = 101$, the steps and oscillations are large but become smaller as the system size increases as shown in Fig. 2 for $N = 201$. But they disappear in the limit $N \rightarrow \infty$. To examine the different behavior of the concurrence for the Ising model and the XY model, we took the system size to be infinite, $N \rightarrow \infty$, where the two models have exact solutions. However, the behavior is the same for a finite system with $N = 201$. For larger values of i_m the concurrence gets larger and approaches its maximum value, the pure case with $\alpha = 0$, at large values $i_m \gg 1$. It is worth mentioning that, for the Ising model, the range of entanglement [63], which is the maximum distance between spins at which the concurrence is different from zero, vanishes unless the two sites are at most next-nearest neighbors. For $\gamma \neq 1$, the range of entanglement is not universal and tends to infinity as γ tends to zero.

So far we have examined the change of entanglement as the degree of the anisotropy γ varies between zero and one and by introducing impurities at fixed sites. Rather than locating the impurity at one site in the chain, we can also introduce a Gaussian distribution of the disorder near a particular location [62]. This can be done by modifying α , the exchange interaction, where α introduces the impurity in a Gaussian form centered at $(N + 1)/2$ with strength or height ζ :

$$\alpha_{i,i+1} = \zeta e^{-\epsilon(i-(N+1)/2)^2} \quad (44)$$

The external magnetic field can also be modified to take the form $h_i = h(1 + \beta_i)$, where β has the following Gaussian distribution [62]:

$$\beta_i = \zeta e^{-\epsilon(i-(N+1)/2)^2} \quad (45)$$

where ϵ is a parameter to be fixed. Numerical calculations show that the entanglement can be tuned in this case by varying the strengths of the magnetic field and the impurity distribution in the system. The concurrence is maximum close to λ_c and can be tuned to zero above the critical point.

F. Thermal Entanglement and the Effect of Temperature

Recently, the concept of thermal entanglement was introduced and studied within one-dimensional spin systems [64–66]. The state of the system described by the Hamiltonian H at thermal equilibrium is $\rho(T) = \exp(-H/kT)/Z$, where $Z = \text{Tr}[\exp(-H/kT)]$ is the partition function and k is Boltzmann's constant. As $\rho(T)$ represents a thermal state, the entanglement in the state is called the thermal entanglement [64].

For a two-qubit isotropic Heisenberg model, there exists thermal entanglement for the antiferromagnetic case and no thermal entanglement for the

ferromagnetic case [64]; while for the XY model the thermal entanglement appears for both the antiferromagnetic and ferromagnetic cases [67, 68]. It is known that the isotropic Heisenberg model and the XY model are special cases of the anisotropic Heisenberg model.

Now that the entanglement of the XY Hamiltonian with impurities has been calculated at $T = 0$, we can consider the case where the system is at thermal equilibrium at temperature T . The density matrix for the XY model at thermal equilibrium is given by the canonical ensemble $\rho = e^{-\beta H} / Z$, where $\beta = 1/k_B T$, and $Z = \text{Tr} (e^{-\beta H})$ is the partition function. The thermal density matrix is diagonal when expressed in terms of the Jordan–Wigner fermionic operators. Our interest lies in calculating the quantum correlations present in the system as a function of the parameters β , γ , λ , and α .

For the pure Ising model with $\alpha = 0$, the constructed two-site density matrices [66] are valid for all temperatures. By using these matrices, it is possible to study the purely two-party entanglement present at thermal equilibrium because the concurrence measure of entanglement can be applied to arbitrary mixed states. For this model the influence that the critical point has on the entanglement structure at nonzero temperatures is particularly clear. The entanglement between nearest-neighbor in the Ising model at nonzero temperature is shown in Fig. 3. The entanglement is nonzero only in a certain region in the $k_B T - \lambda$ plane. It is in this region that quantum effects are likely to dominate the behavior of the system. The entanglement is largest in the vicinity of the critical point $\lambda = 1$, $k_B T = 0$.

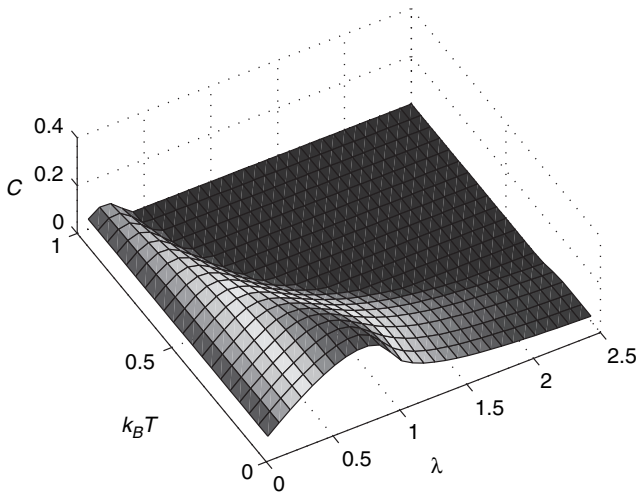


Figure 3. Nearest-neighbor concurrence C at nonzero temperature for the transverse Ising model.

Figure 3 shows that, for certain values of λ , the two-site entanglement can increase as the temperature is increased. Moreover, it shows the existence of appreciable entanglement in the system for temperatures $k_B T$ above the ground-state energy gap Δ . It has been argued that quantum systems behave classically when the temperature exceeds all relevant frequencies. For the transverse Ising model, the only relevant frequency is given by the ground-state energy gap $\Delta \equiv \hbar\omega$. The presence of entanglement in the system for temperatures above the energy gap indicates that quantum effects may persist past the point where they are usually expected to disappear.

The zero-temperature calculations of the previous section Section, the XY model with impurities, represent a highly idealized situation; however, it is unclear whether they have any relevance to the system at nonzero temperature. Since the properties of a quantum system for low temperatures are strongly influenced by nearby quantum critical points, it is tempting to attribute the effect of nearby critical points to persistent mixed-state entanglement in the thermal state.

G. Entanglement for Two-Dimensional Spin Systems

Quantum spin systems in two-dimensional lattices have been the subject of intense research, mainly motivated by their possible relevance in the study of high-temperature superconductors [69]. On the other hand, high magnetic field experiments on materials with a two-dimensional structure, which can be described by the Heisenberg antiferromagnetic model in frustrated lattices, have revealed novel phases as plateaus and jumps in the magnetization curves [70] and might be useful for quantum computations. Among the many different techniques that have been used to study such systems, the generalization of the celebrated Jordan–Wigner transformation [71] to two spatial dimensions [72] has some appealing features. It allows one to write the spin Hamiltonian completely in terms of spinless fermions in such a way that the $S = \frac{1}{2}$ single-particle constraint is automatically satisfied due to the Pauli principle, while the magnetic field enters as the chemical potential for the Jordan–Wigner fermions. This method has been applied to study the XXZ Heisenberg antiferromagnet [73–75].

For this case one can use the Jordan–Wigner transformation since it is a generalization of the well-known transformation in one dimension that we have used in previous sections. The Jordan–Wigner transformation is exact but the resulting Hamiltonian is highly nonlocal and some kind of approximation is necessary to proceed. One can use numerical methods such as Monte Carlo and variational approach to deal with the transformed Hamiltonian. This will allow us to explore the ground state of two-dimensional lattice spin $\frac{1}{2}$ systems, in a way that could be applied to arbitrary lattice topologies. The method can also be used in the presence of an external magnetic field, at finite temperature, and can even be

applied to disordered systems. Once this is solved and we have the density matrix, we can follow the previous procedure to examine the entanglement as the parameters of external magnetic field, temperature, lattice topologies, and impurities vary.

III. ENTANGLEMENT FOR QUANTUM DOT SYSTEMS

A. Two-Electron Two-Site Hubbard Model

Many electron systems such as molecules and quantum dots show the complex phenomena of electron correlation caused by Coulomb interactions. These phenomena can be described to some extent by the Hubbard model [76]. This is a simple model that captures the main physics of the problem and admits an exact solution in some special cases [77]. To calculate the entanglement for electrons described by this model, we will use Zanardi's measure, which is given in Fock space as the von Neumann entropy [78].

1. Exact Solution

The Hamiltonian of the two-electron two-site Hubbard model can be written [77]

$$H = -\frac{t}{2} \sum_{i,\sigma} c_{i\sigma}^\dagger c_{i\bar{\sigma}} + 2U \sum_i \hat{n}_{i\uparrow} \hat{n}_{i\downarrow} \quad (46)$$

where $c_{i\sigma}^\dagger$ and $c_{i\sigma}$ are the Fermi creation and annihilation operators at site i and with spin $\sigma = \uparrow, \downarrow$ and $\hat{n}_{i\sigma} = c_{i\sigma}^\dagger c_{i\sigma}$ is the spin-dependent occupancy operator at site i . For a two-site system $i = 1$ and 2 , $\bar{i} = 3 - i$, $t/2$ is the hopping term of different sites, and $2U$ is the on-site interaction ($U > 0$ for repulsion in our case). The factors $t/2$ and $2U$ are chosen to make the following expressions for eigenvalues and eigenvectors as simple as possible. This Hamiltonian can be solved exactly in the basis set $|1 \uparrow, 1 \downarrow, 2 \uparrow, 2 \downarrow\rangle$; it is simply a (4×4) matrix of the form

$$H = \begin{pmatrix} 2U & -t/2 & -t/2 & 0 \\ -t/2 & 0 & 0 & -t/2 \\ -t/2 & 0 & 0 & -t/2 \\ 0 & -t/2 & -t/2 & 2U \end{pmatrix} \quad (47)$$

with the following four eigenvalues and eigenvectors,

$$\lambda_1 = U - \sqrt{t^2 + U^2}, \quad \lambda_2 = 0, \quad \lambda_3 = 2U, \quad \lambda_4 = U + \sqrt{t^2 + U^2} \quad (48)$$

and the corresponding eigenvectors,

$$|\phi_1\rangle = \begin{pmatrix} 1 \\ x + \sqrt{1+x^2} \\ x + \sqrt{1+x^2} \\ 1 \end{pmatrix}, \quad |\phi_2\rangle = \begin{pmatrix} 0 \\ -1 \\ 1 \\ 0 \end{pmatrix}, \quad (49)$$

$$|\phi_3\rangle = \begin{pmatrix} -1 \\ 0 \\ 0 \\ 1 \end{pmatrix}, \quad |\phi_4\rangle = \begin{pmatrix} 1 \\ x - \sqrt{1+x^2} \\ x - \sqrt{1+x^2} \\ 1 \end{pmatrix} \quad (50)$$

with $x = U/t$. The eigenvalue and eigenvector for the ground state are

$$E = U - \sqrt{t^2 + U^2} \quad (51)$$

and

$$|GS\rangle = |1, x + \sqrt{1+x^2}, x + \sqrt{1+x^2}, 1\rangle \quad (52)$$

2. Hartree–Fock Approximation

In quantum chemistry, the correlation energy E_{corr} is defined as $E_{\text{corr}} = E_{\text{exact}} - E_{\text{HF}}$. In order to calculate the correlation energy of our system, we show how to calculate the ground state using the Hartree–Fock approximation. The main idea is to expand the exact wavefunction in the form of a configuration interaction picture. The first term of this expansion corresponds to the Hartree–Fock wavefunction. As a first step we calculate the spin-traced one-particle density matrix [5] (1PDM) γ :

$$\gamma_{ij} = \langle GS | \sum_{\sigma} c_{i\sigma}^{\dagger} c_{j\sigma} | GS \rangle \quad (53)$$

We obtain

$$\gamma = \begin{pmatrix} 1 & 2\alpha\beta \\ 2\alpha & 1 \end{pmatrix} \quad (54)$$

where

$$\alpha = \frac{1}{\sqrt{2}} \sqrt{1 - \frac{x}{1+x^2}} \quad \text{and} \quad \beta = \frac{1}{\sqrt{2}} \sqrt{1 + \frac{x}{1+x^2}}$$

Diagonalizing this 1PDM, we can get the binding (+) and unbinding (−) molecular natural orbitals (NOs),

$$|\pm\rangle = \frac{1}{\sqrt{2}}(|1\rangle \pm |2\rangle) \quad (55)$$

and the corresponding eigenvalues

$$n_{\pm} = 1 \pm \frac{1}{\sqrt{1+x^2}} \quad (56)$$

where $|1\rangle$ and $|2\rangle$ are the spatial orbitals of sites 1 and 2, respectively. The NOs for different spins are defined as

$$|\pm\sigma\rangle = \frac{1}{\sqrt{2}}(c_{1\sigma}^{\dagger} \pm c_{2\sigma}^{\dagger})|0\rangle \equiv c_{\pm\sigma}^{\dagger}|0\rangle \quad (57)$$

where $|0\rangle$ is the vacuum state. After we define the geminals $|\pm\pm\rangle = c_{\pm\uparrow}^{\dagger}c_{\pm\downarrow}^{\dagger}|0\rangle$, we can express $|GS\rangle$ in terms of NOs as

$$|GS\rangle = \sqrt{\frac{n_+}{2}}|++\rangle - \text{sgn } U \sqrt{\frac{n_-}{2}}|--\rangle \quad (58)$$

In the Hartree–Fock approximation, the GS is given by $|HF\rangle = |++\rangle$ and $E_{HF} = -t + U$. Let us examine the Hartree–Fock results by defining the ionic and nonionic geminals, respectively:

$$\begin{aligned} |A\rangle &= \frac{1}{\sqrt{2}}(c_{1\uparrow}^{\dagger}c_{1\downarrow}^{\dagger} + c_{2\uparrow}^{\dagger}c_{2\downarrow}^{\dagger})|0\rangle \\ |B\rangle &= \frac{1}{\sqrt{2}}(c_{1\uparrow}^{\dagger}c_{2\downarrow}^{\dagger} + c_{2\uparrow}^{\dagger}c_{1\downarrow}^{\dagger})|0\rangle \end{aligned} \quad (59)$$

If $x \rightarrow 0$, the system is equally mixed between ionic and nonionic geminal, $|HF\rangle = |A\rangle + |B\rangle$. When $x \rightarrow +\infty$, $|GS\rangle \rightarrow |B\rangle$, which indicates that as x becomes large, our system goes to the nonionic state. Similarly, $|GS\rangle \rightarrow |C\rangle$, as $x \rightarrow -\infty$, where

$$|C\rangle = \frac{1}{\sqrt{2}}(c_{1\uparrow}^{\dagger}c_{1\downarrow}^{\dagger} - c_{2\uparrow}^{\dagger}c_{2\downarrow}^{\dagger})|0\rangle$$

Thus the HF results are a good approximation only when $x \rightarrow 0$. The unreasonable diverging behavior results from not suppressing the ionic state $|A\rangle$ in $|HF\rangle$

when $|x| \rightarrow \infty$. In order to correct this shortcoming of the Hartree–Fock method, we can combine different wavefunctions in different ranges to obtain a better wavefunction for our system. This can be done as follows:

Range	GS Energy	Correlation Energy	Wavefunction	\mathbf{n}_+	\mathbf{n}_-
$U > t$	0	$U - \sqrt{U^2 + t^2}$	$ B\rangle$	1	1
$-t \geq U \geq t$	$-t + U$	$t - \sqrt{U^2 + t^2}$	$\frac{1}{\sqrt{2}}(A\rangle + B\rangle)$	2	0
$U < -t$	$2U$	$-U - \sqrt{U^2 + t^2}$	$ C\rangle$	1	1

3. Correlation Entropy

The correlation entropy is a good measure of electron correlation in molecular systems [5, 7]. It is defined using the eigenvalues n_k of the one-particle density matrix 1PDM,

$$S = \sum_k n_k (-\ln n_k), \quad \sum_k n_k = N \quad (60)$$

This correlation entropy is based on the nonidempotency of the NONs n_k and proves to be an appropriate measure of the correlation strength if the reference state defining correlation is a single Slater determinant. In addition to the eigenvalues n_k of the “full” (spin-dependent) 1PDM, it seems reasonable to consider also the eigenvalues n_k of the spin-traced 1PDM. Among all the n_k there are a certain number N_0 of NONs n_{k_0} with values between 1 and 2 and all the other N_1 NONs n_{k_1} also have values between 0 and 1. So one possible measure of the correlation strength of spin-traced 1PDM is

$$S_1 = - \sum_{k_0} (n_{k_0} - 1) \ln(n_{k_0} - 1) - \sum_{k_1} n_{k_1} \ln n_{k_1} \quad (61)$$

Since all the $n_k/2$ have values between 0 and 1, there is another possible measurement of the correlation strength:

$$S_2 = - \sum_k \frac{n_k}{2} \ln \frac{n_k}{2} \quad (62)$$

4. Entanglement

The entanglement measure is given by the von Neumann entropy [78]

$$E_j = -\text{Tr}(\rho_j \log_2 \rho_j), \quad \rho_j = \text{Tr}_j(|\Psi\rangle\langle\Psi|) \quad (63)$$

where Tr_j denotes the trace over all but the j th site, $|\Psi\rangle$ is the antisymmetric wavefunction of the fermions system, and ρ_j is the reduced density matrix. Hence E_j actually describes the entanglement of the j th site with the remaining sites [79].

In the Hubbard model, the electron occupation of each site has four possibilities; there are four possible local states at each site, $|v\rangle_j = |0\rangle_j, |\uparrow\rangle_j, |\downarrow\rangle_j, |\uparrow\downarrow\rangle_j$. The reduced density matrix of the j th site with the other sites is given by [80, 81]

$$\rho_j = z|0\rangle\langle 0| + u^+|\uparrow\rangle\langle\uparrow| + u^-|\downarrow\rangle\langle\downarrow| + w|\uparrow\downarrow\rangle\langle\uparrow\downarrow| \quad (64)$$

with

$$w = \langle n_{j\uparrow}n_{j\downarrow} \rangle = \text{Tr}(n_{j\uparrow}n_{j\downarrow}\rho_j) \quad (65)$$

$$u^+ = \langle n_{j\uparrow} \rangle - w, \quad u^- = \langle n_{j\downarrow} \rangle - w \quad (66)$$

$$z = 1 - u^+ - u^- - w = 1 - \langle n_{j\uparrow} \rangle - \langle n_{j\downarrow} \rangle + w \quad (67)$$

And the entanglement between the j th site and other sites is given by

$$E_j = -z \text{Log}_2 z - u^+ \text{Log}_2 u^+ - u^- \text{Log}_2 u^- - w \text{Log}_2 w \quad (68)$$

For the one-dimensional Hubbard model with half-filling electrons, we have $\langle n_{j\uparrow} \rangle = \langle n_{j\downarrow} \rangle = \frac{1}{2}$, $u^+ = u^- = \frac{1}{2} - w$, and the entanglement is given by

$$E_j = -2w \text{log}_2 w - 2\left(\frac{1}{2} - w\right) \text{log}_2 \left(\frac{1}{2} - w\right) \quad (54)$$

For our case of a two-site two-electron system

$$w = \frac{1}{2 + 2[x + \sqrt{1 + x^2}]^2}$$

Thus the entanglement is readily calculated from Eq. (69). In Fig. 4, we show the entanglement between the two sites (top curve) and the correlation entropy S_1 and S_2 as a function of $x = U/t$. The entanglement measure is given by the von Neumann entropy in which the density matrix of the system is traced over the other site to get the reduced density matrix. The reduced density matrix describes the four possible occupations on the site: $|0\rangle, |\uparrow\rangle, |\downarrow\rangle, |\uparrow\downarrow\rangle$. The minimum of the entanglement is 1 as $x \rightarrow \pm\infty$. It can be understood that when $U \rightarrow +\infty$, all the sites are singly occupied; the only difference is the spin of the electrons at each site, which can be referred to as spin entanglement. As $U \rightarrow -\infty$, all the sites are either doubly occupied or empty, which is referred to as space entanglement. The maximum of the entanglement is 2 at $U = 0$; all four

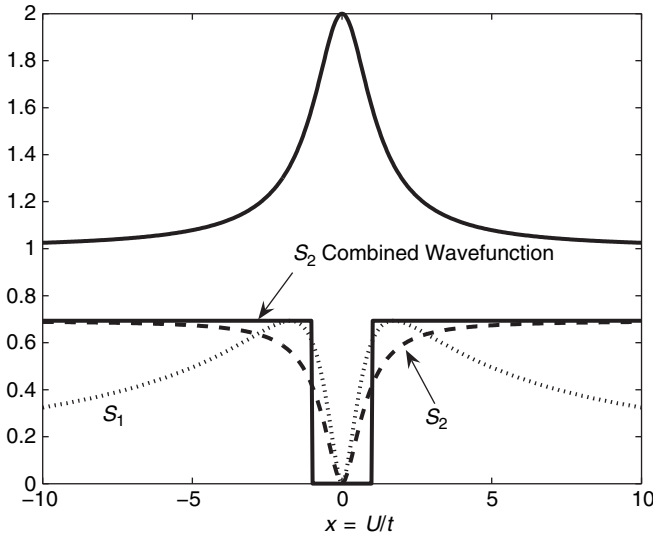


Figure 4. Two-site Hubbard model. Upper curve is the entanglement calculated by the von Neumann entropy. The curves S_1 and S_2 are the correlation entropies of the exact wavefunction as defined in the text. The dashed line is the S_2 for the combined wavefunction based on the range of x values. S_1 for the combined wavefunction is zero.

occupations are evenly weighted, which is the sum of the spin and space entanglements of the system. The correlation entropy S_1 vanishes for $x \rightarrow 0$ and $x \rightarrow \pm\infty$ and has a maximum near $|x| = 1$; the correlation entropy S_2 vanishes for $x \rightarrow 0$ and increases monotonically and approaches $\ln 2$ for $x \rightarrow \pm\infty$. For $x \rightarrow +\infty$ it can be viewed as $t \rightarrow 0$ for fixed $U > 0$ or as $U \rightarrow +\infty$ for fixed t .

B. One-Dimensional Quantum Dots System

We consider an array of quantum dots modeled by the one-dimensional Hubbard Hamiltonian of the form [82]

$$H = - \sum_{\langle ij \rangle, \sigma} t_{ij} c_{i\sigma}^{\dagger} c_{j\sigma} + U \sum_i n_{i\uparrow} n_{i\downarrow} \quad (70)$$

where t_{ij} stands for the hopping between the nearest-neighbor sites for the electrons with the same spin, i and j are the neighboring site numbers, σ is the electron spin, $c_{i\sigma}^{\dagger}$ and $c_{j\sigma}$ are the creation and annihilation operators, and U is the Coulomb repulsion for the electrons on the same site. The periodic boundary condition is applied. The entanglement measure is given by the von Neumann entropy [78].

In the Hubbard model, the electron occupation of each site has four possibilities; there are four possible local states at each site, $|v\rangle_j = |0\rangle_j, |\uparrow\rangle_j, |\downarrow\rangle_j, |\uparrow\downarrow\rangle_j$. The dimensions of the Hilbert space of an L -site system is 4^L and $|v_1 v_2 \cdots v_L\rangle = \prod_{j=1}^L |v_j\rangle_j$ can be used as basis vectors for the system. The entanglement of the j th site with the other sites is given in the previous section by Eq. (65).

In the ideal case, we can expect an array of the quantum dots to have the same size and to be distributed evenly, so that the parameters t and U are the same everywhere. We call this the pure case. In fact, the size of the dots may not be the same and they may not be evenly distributed, which we call the impurity case. Here, we consider two types of impurities. The first one is to introduce a symmetric hopping impurity t' between two neighboring dots; the second one is to introduce an asymmetric electron hopping t' between two neighboring dots, the right hopping is different from the left hopping, while the rest of the sites have hopping parameter t .

Consider the particle-hole symmetry of the one-dimensional Hubbard model. One can obtain $w(-U) = \frac{1}{2} - w(U)$, so the entanglement is an even function of U , $E_j(-U) = E_j(U)$. The minimum of the entanglement is 1 as $U \rightarrow \pm\infty$. As $U \rightarrow +\infty$, all the sites are singly occupied; the only difference is the spin of the electrons on each site, which can be referred to as spin entanglement. As $U \rightarrow -\infty$, all the sites are either doubly occupied or empty, which is referred to as space entanglement. The maximum of the entanglement is 2 at $U = 0$, which is the sum of the spin and space entanglements of the system. The ground state of the one-dimensional Hubbard model at half-filling is metallic for $U < 0$, and insulating for $U > 0$; $U = 0$ is the critical point for the metal-insulator transition, where the local entanglement reaches its maximum. In Fig. 5 we show the

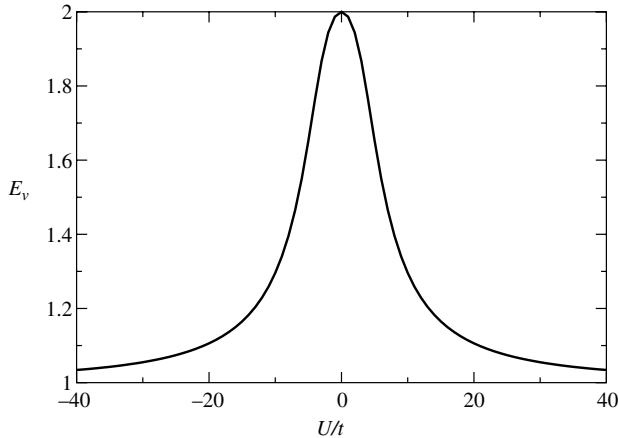


Figure 5. Local entanglement given by the von Neumann entropy, E_v , versus U/t in the pure case.

entanglement as a function U/t for six sites and six electrons. Our results are in complete agreement with the exact one obtained by Bethe ansatz [80].

C. Two-Dimensional Array of Quantum Dots

Using the Hubbard model, we can study the entanglement scaling behavior in a two-dimensional itinerant system. Our results indicate that, on the two sides of the critical point denoting an inherent quantum phase transition (QPT), the entanglement follows different scalings with the size just as an order parameter does. This fact reveals the subtle role played by the entanglement in QPT and points to its potential application in quantum information processing as a fungible physical resource.

Recently, it has been speculated that the most entangled systems could be found at the critical point [83] when the system undergoes a quantum phase transition; that is, a qualitative change of some physical properties takes place as an order parameter in the Hamiltonian is tuned [84]. QPT results from quantum fluctuations at the absolute zero of temperature and is a pure quantum effect featured by long-range correlations. So far, there have already been some efforts in exploring the above speculations, such as the analysis of the XY model about the single-spin entropies and two-spin quantum correlations [59, 85], the entanglement between a block of L contiguous sites and the rest of the chain [51], and also the scaling of entanglement near QPT [60]. But because there is still no analytical proof, the role played by the entanglement in quantum critical phenomena remains elusive. Generally, at least two difficulties exist in resolving this issue. First, until now, only two-particle entanglement is well explored. How to quantify the multiparticle entanglement is not clear. Second, QPT closely relates to the notorious many-body problems, which is almost intractable analytically. Until now, the only effective and accurate way to deal with QPT in critical region is the density-matrix renormalization group method [86]. Unfortunately, it is only efficient for one-dimensional cases because of the much more complicated boundary conditions for the two-dimensional situation [87].

In this chapter, we will focus on the entanglement behavior in QPT for the two-dimensional array of quantum dots, which provide a suitable arena for implementation of quantum computation [88, 89, 103]. For this purpose, the real-space renormalization group technique [91] will be utilized and developed for the finite-size analysis of entanglement. The model that we will be using is the Hubbard model [83],

$$H = -t \sum_{\langle i,j \rangle, \sigma} [c_{i\sigma}^+ c_{j\sigma} + \text{h.c.}] + U \sum_i \left(\frac{1}{2} - n_{i\uparrow}\right) \left(\frac{1}{2} - n_{i\downarrow}\right) \quad (71)$$

where t is the nearest-neighbor hopping term and U is the local repulsive interaction. $c_{i\sigma}^+$ ($c_{i\sigma}$) creates (annihilates) an electron with spin σ in a Wannier orbital

located at site i ; the corresponding number operator is $n_{i\sigma} = c_{i\sigma}^\dagger c_{i\sigma}$ and $\langle \rangle$ denotes the nearest-neighbor pairs; h.c. denotes the Hermitian conjugate.

For a half-filled triangular quantum lattice, there exists a metal–insulator phase transition with the tuning parameter U/t at the critical point 12.5 [92–94]. The corresponding order parameter for metal–insulator transition is the charge gap defined by $\Delta_g = E(N_e - 1) + E(N_e + 1) - 2E(N_e)$, where $E(N_e)$ denotes the lowest energy for an N_e -electron system. In our case, N_e is equal to the site number N_s of the lattice. Unlike the charge gap calculated from the energy levels, the Zanardi measure of the entanglement is defined based on the wavefunction corresponding to $E(N_e)$ instead. Using the conventional renormalization group method for the finite-size scaling analysis [92–94], we can discuss three schemes of entanglement scaling: single-site entanglement scaling with the total system size, E_{single} ; single-block entanglement scaling with the block size, E_{block} ; and block–block entanglement scaling with the block size, $E_{\text{block–block}}$. Our initial results of the single-site entanglement scaling indicate that E_{single} is not a universal quantity. This conclusion is consistent with the argument given by Osborne and Nielsen [85], who claim that the single-site entanglement is not scalable because it does not have the proper extensivity and does not distinguish between the local and the distributed entanglement. This implies that only a limited region of sites around the central site contributed significantly to the single-site entanglement. Using the one-parameter scaling theory, near the phase transition point, we can assume the existence of scaling function f for $E_{\text{block–block}}$ such that $E_{\text{block–block}} = q^{\nu_E} f(L/\xi)$, where $q = (U/t) - (U/t)_c$ measures the deviation distance of the system away from the critical state with $(U/t)_c = 12.5$, which is exactly equal to the critical value for metal–insulator transition when the same order parameter U/t is used [92–94]. $\xi = q^{-\nu}$ is the correlation length of the system with the critical exponent ν and $N = L^2$ for the two-dimensional systems.

In Fig. 6, we show the results of $E_{\text{block–block}}$ as a function of (U/t) for different system sizes. With proper scaling, all the curves collapse into one curve, which can be expressed as $E_{\text{block–block}} = f(qN^{1/2})$. Thus the critical exponents are $\nu_E = 0, \nu = 1$. It is interesting to note that we obtained the same ν as in the study of the metal–insulator transition. This shows the consistency of the initial results since the critical exponent ν is only dependent on the inherent symmetry and dimension of the investigated system. Another significant result lies in the finding that the metal state is highly entangled while the insulating state is only partly entangled.

It should be mentioned that the calculated entanglement here has a corresponding critical exponent $\nu_E = 0$. This means that the entanglement is constant at the critical point over all sizes of the system. But it is not a constant over all values of U/t . There is an abrupt jump across the critical point as $L \rightarrow \infty$. If we divide the regime of the order parameter into noncritical regime and critical

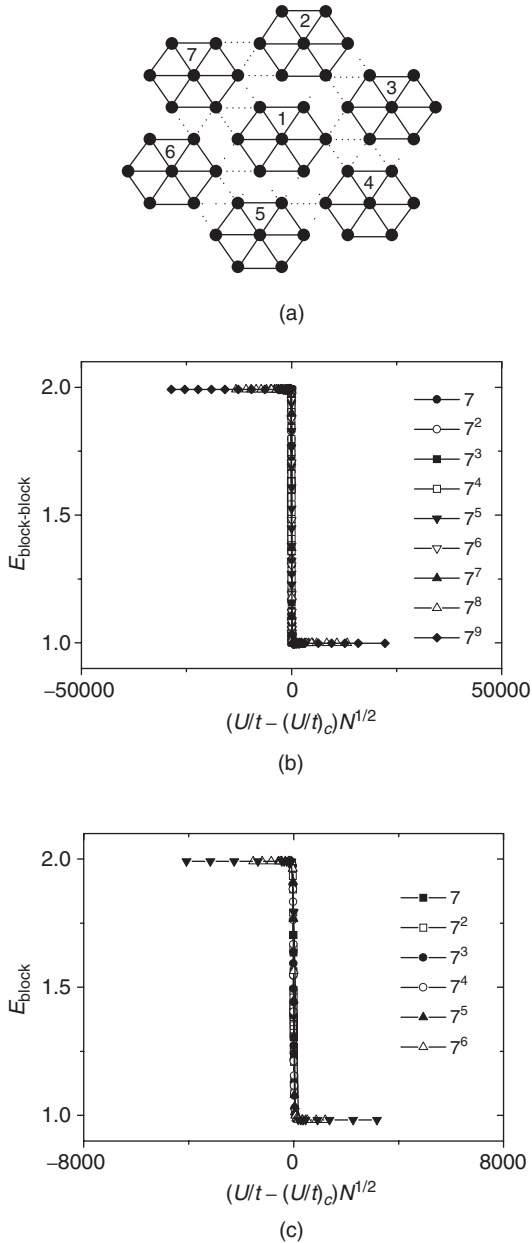


Figure 6. (a) Schematic diagram displays the lattice configuration with central block and the surrounding ones. (b) Scaling of block–block for various system size and (c) scaling of block entanglements with the block size.

regime, the results can be summarized as follows. In the noncritical regime, that is, U/t is away from $(U/t)_c$, as L increases, the entanglement will saturate onto two different values depending on the sign of $U/t - (U/t)_c$; at the critical point, the entanglement is actually a constant independent of the size L . These properties are qualitatively different from the single-site entanglement discussed by Osborne and Nielsen [85], where the entanglement with Zanardi's measure increases from zero to the maximum at the critical point and then decreases again to zero as the order parameter γ for the XY mode is tuned. These peculiar properties of the entanglement found here can be of potential interest to make an effective ideal "entanglement switch." For example, with seven blocks of quantum dots on a triangular lattice, the entanglement among the blocks can be regulated as "0" or "1" almost immediately once the tuning parameter U/t crosses the critical point. The switch errors will depend on the size of the blocks. Since it is already a well-developed technique to change U/t for the quantum dot lattice [95, 103], the above scheme should be workable. To remove the special confinement we have made upon the calculated entanglement, namely, only the entanglement of blocks 1 and 7 with the rest ones are considered, in the following, we will prove that the average pairwise entanglement also has the properties shown in Fig. 6. As we change the size of the central block, its entanglement with all the rest of the sites follows the same scaling properties as $E_{\text{block-block}}$. It is understandable if we consider the fact that only a limited region round the block contributes mostly to E_{block} . This result greatly facilitates the fabrication of realistic entanglement control devices, such as quantum gates for a quantum computer, since we don't need to consider the number of component blocks in fear that the next neighboring or the next-next neighboring quantum dots will influence the switching effect.

IV. AB INITIO CALCULATIONS AND ENTANGLEMENT

For a two-electron system in $2m$ -dimensional spin-space orbital, with c_a and c_a^\dagger denoting the fermionic annihilation and creation operators of single-particle states and $|0\rangle$ representing the vacuum state, a pure two-electron state $|\Phi\rangle$ can be written [57]

$$|\Phi\rangle = \sum_{a,b \in \{1,2,3,4,\dots,2m\}} \omega_{a,b} c_a^\dagger c_b^\dagger |0\rangle \quad (72)$$

where a, b run over the orthonormal single-particle states, and Pauli exclusion requires that the $2m \times 2m$ expansion coefficient matrix ω is antisymmetric: $\omega_{a,b} = -\omega_{b,a}$, and $\omega_{i,i} = 0$.

In the occupation number representation $(n_1 \uparrow, n_1 \downarrow, n_2 \uparrow, n_2 \downarrow, \dots, n_m \uparrow, n_m \downarrow)$, where \uparrow and \downarrow mean α and β electrons, respectively, the subscripts

denote the spatial orbital index and m is the total spatial orbital number. By tracing out all other spatial orbitals except n_1 , we can obtain a (4×4) reduced density matrix for the spatial orbital n_1

$$\begin{aligned} \rho_{n_1} &= \text{Tr}_{n_1} |\Phi\rangle\langle\Phi| \\ &= \begin{pmatrix} 4 \sum_{i,j=1}^{m-1} |\omega_{2i+1,2j+2}|^2 & 0 & 0 & 0 \\ 0 & 4 \sum_{i=1}^{m-1} |\omega_{2,2i+1}|^2 & 0 & 0 \\ 0 & 0 & 4 \sum_{i=2}^m |\omega_{1,2i}|^2 & 0 \\ 0 & 0 & 0 & 4|\omega_{1,2}|^2 \end{pmatrix} \end{aligned} \quad (73)$$

The matrix elements of ω can be calculated from the expansion coefficient of the ab initio configuration interaction method. The CI wavefunction with single and double excitations can be written

$$|\Phi\rangle = c_0 |\Psi_0\rangle + \sum_{ar} c_a^r |\Psi_a^r\rangle + \sum_{a<b,r<s} c_{a,b}^{r,s} |\Psi_{a,b}^{r,s}\rangle \quad (74)$$

where $|\Psi_0\rangle$ is the ground-state Hartree–Fock wavefunction, c_a^r is the coefficient for single excitation from orbital a to r , and $c_{a,b}^{r,s}$ is the double excitation from orbital a and b to r and s . Now the matrix elements of ω can be written in terms of the CI expansion coefficients. In this general approach, the ground-state entanglement is given by the von Neumann entropy of the reduced density matrix ρ_{n_1} [57]:

$$S(\rho_{n_1}) = -\text{Tr}(\rho_{n_1} \log_2 \rho_{n_1}) \quad (75)$$

We are now ready to evaluate the entanglement for the H_2 molecule [57] as a function of R using a two-electron density matrix calculated from the configuration interaction wavefunction with single and double electronic excitations [96]. Figure 7 shows the calculated entanglement S for the H_2 molecule, as a function of the internuclear distance R using a minimal Gaussian basis set STO-3G (each Slater-type orbital fitted by 3 Gaussian functions) and a split valence Gaussian basis set 3-21G [96]. For comparison we included the usual electron correlation ($E_c = |E^{\text{exact}} - E^{\text{UHF}}|$) and spin-unrestricted Hartree–Fock (UHF) calculations [96] using the same basis set in the figure. At the limit $R = 0$, the electron correlation for the He atom, $E_c = 0.0149$ (au) using the 3-21G basis set compared with the entanglement for the He atom $S = 0.0313$. With a larger basis set, $cc - pV5Z$ [97], we obtain numerically $E_c = 0.0415$ (au) and $S = 0.0675$. Thus qualitatively entanglement and absolute correlation have similar behavior.

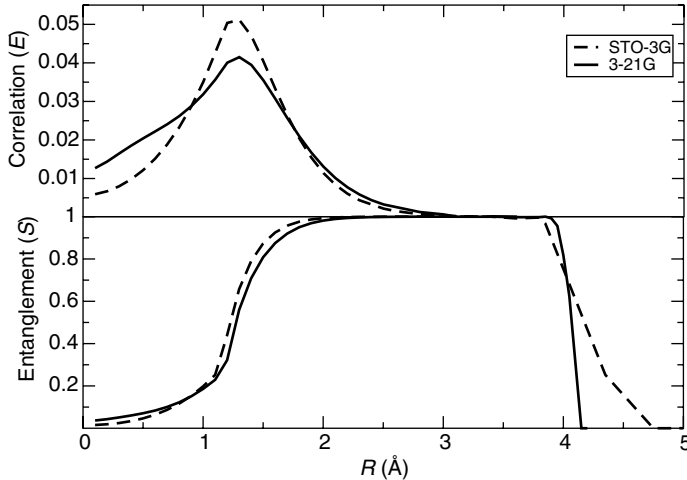


Figure 7. Comparison between the absolute value of the electron correlation $E_c = |E^{\text{Exact}} - E^{\text{UHF}}|$ and the von Neumann entropy (S) as a function of the internuclear distance R for the H_2 molecule using two Gaussian basis sets STO-3G and 3-21G.

At the united atom limit, $R \rightarrow 0$, both have small values, then rise to a maximum value, and finally vanish at the separated atom limit, $R \rightarrow \infty$. However, note that for $R > 3$ Å the correlation between the two electrons is almost zero but the entanglement is maximal until around $R \sim 4$ Å; the entanglement vanishes for $R > 4$ Å.

V. DYNAMICS OF ENTANGLEMENT AND DECOHERENCE

In this section, we investigate the dynamics of entanglement in one-dimensional spin systems with a time-dependent magnetic field. The Hamiltonian for such a system is given by [98]

$$H = -\frac{J}{2}(1 + \gamma) \sum_{i=1}^N \sigma_i^x \sigma_{i+1}^x - \frac{J}{2}(1 - \gamma) \sum_{i=1}^N \sigma_i^y \sigma_{i+1}^y - \sum_{i=1}^N h(t) \sigma_i^z \quad (76)$$

where J is the coupling constant, $h(t)$ is the time-dependent external magnetic field, σ^a are the Pauli matrices ($a = x, y, z$), γ is the degree of anisotropy, and N is the number of sites. We can set $J = 1$ for convenience and use periodic boundary conditions. Next, we transform the spin operators into fermionic operators. So the Hamiltonian assumes the following form:

$$H = \sum_{p=1}^{N/2} \alpha_p(t) [c_p^+ c_p + c_{-p}^+ c_{-p}] + i\delta_p [c_p^+ c_{-p}^+ + c_p c_{-p}] + 2h(t) = \sum_{p=1}^{N/2} \tilde{H}_p \quad (77)$$

where $\alpha_p(t) = -2 \cos \phi_p - 2h(t)$, $\delta_p = 2\gamma \sin \phi_p$, and $\phi_p = 2\pi p/N$. It is easy to show $[\tilde{H}_p, \tilde{H}_q] = 0$, which means the space of \tilde{H} decomposes into noninteracting subspace, each of four dimensions. No matter what $h(t)$ is, there will be no transitions among those subspaces. Using the following basis for the p th subspace, $(|0\rangle; c_p^+ c_{-p}^+ |0\rangle; c_p^+ |0\rangle; c_{-p}^+ |0\rangle)$, we can explicitly get

$$\tilde{H}_p(t) = \begin{pmatrix} 2h(t) & -i\delta_p & 0 & 0 \\ i\delta_p & -4 \cos \phi_p - 2h(t) & 0 & 0 \\ 0 & 0 & -2 \cos \phi_p & 0 \\ 0 & 0 & 0 & -2 \cos \phi_p \end{pmatrix} \quad (78)$$

We only consider the systems that, at time $t = 0$, are in thermal equilibrium at temperature T . Let $\rho_p(t)$ be the density matrix of the p th subspace; we have $\rho_p(0) = e^{-\beta \tilde{H}_p(0)}$, where $\beta = 1/kT$ and k is Boltzmann's constant. Therefore, using Eq. (78), we have $\rho_p(0)$. Let $U_p(t)$ be the time-evolution matrix in the p th subspace, namely, $(\hbar = 1): i dU_p(t)/dt = U_p(t) \tilde{H}_p(t)$, with the boundary condition $U_p(0) = I$. Now the Liouville equation of this system is

$$i \frac{d\rho(t)}{dt} = [H(t), \rho(t)] \quad (79)$$

which can be decomposed into uncorrelated subspaces and solved exactly. Thus, in the p th subspace, the solution of the Liouville equation is $\rho_p(t) = U_p(t) \rho_p(0) U_p(t)^\dagger$.

As a first step to investigate the dynamics of the entanglement, we can take the magnetic field to be a step function then generalize it to other relevant functional forms such as an oscillating one [98]. Figure 8 shows the results for nearest-neighbor concurrence $C(i, i+1)$ at temperature $T = 0$ and $\gamma = 1$ as a function of the initial magnetic field a for the step function case with final field b . For the $a < 1$ region, the concurrence increases very fast near $b = 1$ and reaches a limit $C(i, i+1) \sim 0.125$ when $b \rightarrow \infty$. It is surprising that the concurrence will not disappear when b increases with $a < 1$. This indicates that the concurrence will not disappear as the final external magnetic field increases at infinite time. It shows that this model is not in agreement with obvious physical intuition, since we expect that increasing the external magnetic field will destroy the spin-spin correlation functions and make the concurrence vanish. The concurrence approaches a maximum $C(i, i+1) \sim 0.258$ at $(a = 1.37, b = 1.37)$ and decreases rapidly as $a \neq b$. This indicates that the fluctuation of the external magnetic field near the equilibrium state will rapidly destroy the entanglement. However, in the region where $a > 2.0$, the concurrence is close to zero when $b < 1.0$ and maximum close to 1. Moreover, it disappear in the limit of $b \rightarrow \infty$.

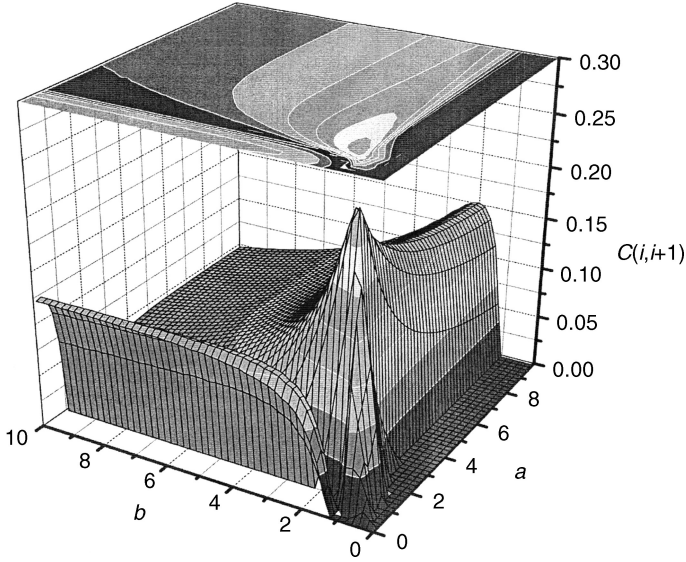


Figure 8. Nearest-neighbor concurrence C at zero temperature as a function of the initial magnetic field a for the step function case with final field b .

Now let us examine the system size effect on the entanglement with three different external magnetic fields changing with time t [99]:

$$h_{\text{I}}(t) = \begin{cases} a, & t \leq 0 \\ b + (a - b)e^{-Kt}, & t > 0 \end{cases} \quad (80)$$

$$h_{\text{II}}(t) = \begin{cases} a, & t \leq 0 \\ a - a \sin(Kt), & t > 0 \end{cases} \quad (81)$$

$$h_{\text{III}}(t) = \begin{cases} 0, & t \leq 0 \\ a - a \cos(Kt), & t > 0 \end{cases} \quad (82)$$

where a , b , and K are varying parameters.

We have found that the entanglement fluctuates shortly after a disturbance by an external magnetic field when the system size is small. For larger system size, the entanglement reaches a stable state for a long time before it fluctuates. However, this fluctuation of entanglement disappears when the system size goes to infinity. We also show that in a periodic external magnetic field, the nearest-neighbor entanglement displays a periodic structure with a period related to that of the magnetic field. For the exponential external magnetic field, by varying the constant K , we have found that as time evolves, $C(i, i + 1)$ oscillates but it does not reach its equilibrium value at $t \rightarrow \infty$.

This confirms the fact that the nonergodic behavior of the concurrence is a general behavior for slowly changing magnetic field. For the periodic magnetic field $h_{\text{II}} = a(1 - \sin(-Kt))$, the nearest-neighbor concurrence is a maximum at $t = 0$ for values of a close to one, since the system exhibits a quantum phase transition at $\lambda_c = J/h = 1$, where in our calculations we fixed $J = 1$. Moreover, for the two periodic $\sin(-Kt)$ and $\cos(-Kt)$ fields the nearest-neighbor concurrence displays a periodic structure according to the periods of their respective magnetic fields [99].

For the periodic external magnetic field $h_{\text{III}}(t)$, we show in Fig. 9 that the nearest-neighbor concurrence $C(i, i + 1)$ is zero at $t = 0$ since the external magnetic field $h_{\text{III}}(t = 0) = 0$ and the spins align along the x -direction: the total wavefunction is factorizable. By increasing the external magnetic field, we see the appearance of nearest-neighbor concurrence but very small. This indicates that the concurrence cannot be produced without a background external magnetic field in the Ising system. However, as time evolves one can see the periodic structure of the nearest-neighbor concurrence according to the periodic structure of the external magnetic field $h_{\text{III}}(t)$ [99].

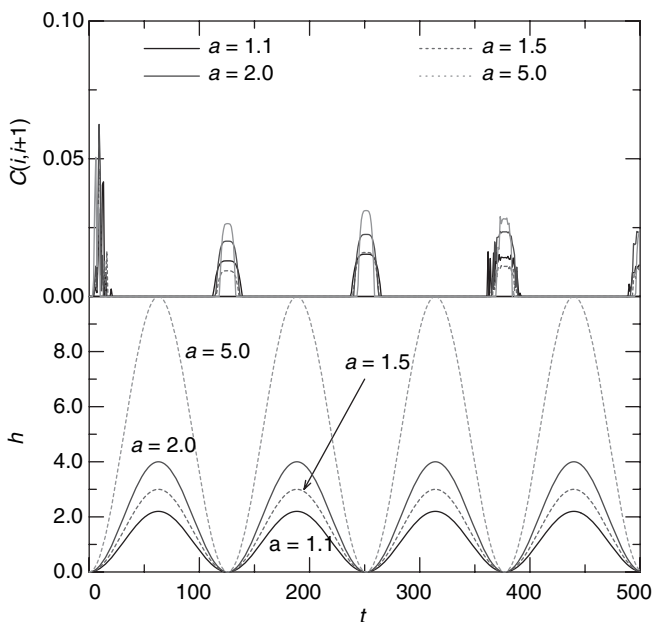


Figure 9. The nearest-neighbor concurrence $C(i, i + 1)$ (upper panel) and the periodic external magnetic field $h_{\text{III}}(t) = a(1 - \cos[Kt])$; see Eq. (14) in the text (lower panel) for $K = 0.05$ with different values of a as a function of time t .

Recently, interest in solid state systems has increased because they facilitate the fabrication of large integrated networks that would be able to implement realistic quantum computing algorithms on a large scale. On the other hand, the strong coupling between a solid state system and its complex environment makes it a significantly challenging mission to achieve the high coherence control required to manipulate the system. Decoherence is considered as one of the main obstacles toward realizing an effective quantum computing system [100–103]. The main effect of decoherence is to randomize the relative phases of the possible states of the isolated system as a result of coupling to the environment. By randomizing the relative phases, the system loses all quantum interference effects and may end up behaving classically.

In order to study the decoherence effect, we examined the time evolution of a single spin coupled by exchange interaction to an environment of interacting spin bath modeled by the XY-Hamiltonian. The Hamiltonian for such a system is given by [104]

$$H = -\frac{1+\gamma}{2} \sum_{i=1}^N J_{i,i+1} \sigma_i^x \sigma_{i+1}^x - \frac{1-\gamma}{2} \sum_{i=1}^N J_{i,i+1} \sigma_i^y \sigma_{i+1}^y - \sum_{i=1}^N h_i \sigma_i^z \quad (83)$$

where $J_{i,i+1}$ is the exchange interaction between sites i and $i+1$, h_i is the strength of the external magnetic field at site i , σ^a are the Pauli matrices ($a = x, y, z$), γ is the degree of anisotropy, and N is the number of sites. We consider the centered spin on the l th site as the single-spin quantum system and the rest of the chain as its environment, where in this case $l = (N+1)/2$. The single spin directly interacts with its nearest-neighbor spins through exchange interaction $J_{l-1,l} = J_{l,l+1} = J'$. We assume exchange interactions between spins in the environment are uniform and simply set it as $J = 1$. The centered spin is considered as inhomogeneously coupled to all the spins in the environment by being directly coupled to its nearest neighbors and indirectly to all other spins in the chain through its nearest neighbors.

By evaluating the spin correlator $C(t)$ of the single spin at the j th site [104],

$$C_j(t) = \rho_j^z(t, \beta) - \rho_j^z(0, \beta) \quad (84)$$

we observed that the decay rate of the spin oscillations strongly depends on the relative magnitude of the exchange coupling between the single spin and its nearest neighbor J' and coupling among the spins in the environment J . The decoherence time varies significantly based on the relative coupling magnitudes of J and J' . The decay rate law has a Gaussian profile when the two exchange couplings are of the same order, $J' \sim J$, but converts to exponential and then a

power law as we move to the regimes of $J' > J$ and $J' < J$. We also show that the spin oscillations propagate from the single spin to the environment spins with a certain speed.

Moreover, the amount of saturated decoherence induced into the spin state depends on this relative magnitude and approaches a maximum value for a relative magnitude of unity. Our results suggest that setting the interaction within the environment in such a way that its magnitude is much higher or lower than the interaction with the single spin may reduce the decay rate of the spin state. The reason behind this phenomenon could be that the variation in the coupling strength along the chain at one point (where the single spin exits) blocks the propagation of decoherence along the chain by reducing the entanglement among the spins within the environment, which reduces its decoherence effect on the single spin in return [104]. This result might be applicable in general to similar cases of a centered quantum system coupled inhomogeneously to an interacting environment with large degrees of freedom.

VI. ENTANGLEMENT AND DENSITY FUNCTIONAL THEORY

Density functional theory is originally based on the Hohenberg–Kohn theorem [105, 106]. In the case of a many-electron system, the Hohenberg–Kohn theorem establishes that the ground-state electronic density $\rho(\mathbf{r})$, instead of the potential $v(\mathbf{r})$, can be used as the fundamental variable to describe the physical properties of the system. In the case of a Hamiltonian given by

$$H = H_0 + H_{\text{ext}} = H_0 + \sum_l \lambda_l \hat{A}_l \quad (85)$$

where λ_l is the control parameter associated with a set of mutually commuting Hermitian operators $\{\hat{A}_l\}$, the expectation values of \hat{A}_l for the ground state $|\psi\rangle$ are denoted by the set $\{a_l\} \equiv \{\langle\psi|\hat{A}_l|\psi\rangle\}$. For such a Hamiltonian Wu et al. [107] linked entanglement in interacting many-body quantum systems to density functional theory. They used the Hohenberg–Kohn theorem on the ground state to show that the ground-state expectation value of any observable can be interchangeably viewed as a unique function of either the control parameter $\{\lambda_l\}$ or the associated operator representing the observable $\{a_l\}$.

The Hohenberg–Kohn theorem can be used to redefine entanglement measures in terms of new physical quantities: expectation values of observables, $\{a_l\}$, instead of external control parameters, $\{\lambda_l\}$. Consider an arbitrary entanglement measure M for the ground state of Hamiltonian (85). For a bipartite entanglement, one can prove a central lemma, which very generally connects M and energy derivatives.

Lemma Any entanglement measure M can be expressed as a unique functional of the set of first derivatives of the ground-state energy [107] :

$$M = M(\{a_l\}) = M\left(\left\{\frac{\partial E}{\partial \lambda_l}\right\}\right) \quad (86)$$

The proof follows from the fact that, according to the generalized Hohenberg–Kohn theorem, the ground-state wavefunction $|\Psi\rangle$ is a unique functional of $\{a_l\}$, and since $|\Psi\rangle$ provides a complete description of the state of the system, everything else is a unique functional of $\{a_l\}$ as well, including M . Wu et al. [107] use density functional theory concepts to express entanglement measures in terms of the first or second derivative of the ground-state energy. As a further application they discuss entanglement and quantum phase transitions in the case of mean field approximations for realistic models of many-body systems [107].

This interesting connection between density functional theory and entanglement was further generalized for arbitrary mixed states by Rajagopal and Rendell [108] using the maximum entropy principle. In this way they established the duality in the sense of Legendre transform between the set of mean values of the observables based on the density matrix and the corresponding set of conjugate control parameters associated with the observables.

VII. FUTURE DIRECTIONS

We have examined and reviewed the relation between electron–electron correlation, the correlation entropy, and the entanglement for two exactly solvable models: the Ising model and the Hubbard model for two sites. The ab initio calculation of the entanglement for the H_2 system is also discussed. Our results show that there is a qualitatively similar behavior between the entanglement and absolute standard correlation of electrons for the Ising model. Thus entanglement might be used as an alternative measure of electron correlation in quantum chemistry calculations. Entanglement is directly observable and it is one of the most striking properties of quantum mechanics.

Dimensional scaling theory [109] provides a natural means to examine electron–electron correlation, quantum phase transitions [110], and entanglement. The primary effect of electron correlation in the $D \rightarrow \infty$ limit is to open up the dihedral angles from their Hartree–Fock values [109] of exactly 90° . Angles in the correlated solution are determined by the balance between centrifugal effects, which always favor 90° , and interelectron repulsions, which always favor 180° . Since the electrons are localized at the $D \rightarrow \infty$ limit, one might need to add the first harmonic correction in the $1/D$ expansion to obtain

a useful density matrix for the whole system, thus the von Neumann entropy. The relation between entanglement and electron–electron correlation at the large-dimensional limit for the dimensional scaling model of the H_2 molecule [111] will be examined in future studies.

A new promising approach is emerging for the realization of quantum chemistry calculations without wavefunctions through first-order semidefinite programming [112]. Mazziotti has developed a first-order, nonlinear algorithm for the semidefinite programming of the two-electron reduced density matrix method that reduces memory and floating-point requirements by orders of magnitude [113, 114]. The electronic energies and properties of atoms and molecules are computable simply from an effective two-electron reduced density matrix $\rho_{(AB)}$ [115, 116]. Thus the electron–electron correlation can be calculated directly as effectively the entanglement between the two electrons, which is readily calculated as the von Neumann entropy $S = -\text{Tr}\rho_A \log_2 \rho_A$, where $\rho_A = \text{Tr}_B \rho_{(AB)}$. With this combined approach, one calculates the electronic energies and properties of atoms and molecules including correlation without wavefunctions or Hartree–Fock reference systems. This approach provides a natural way to extend the calculations of entanglement to larger molecules.

Quantum phase transitions are a qualitative change in the ground state of a quantum many-body system as some parameter is varied [84, 117]. Unlike classical phase transitions, which occur at a nonzero temperature, the fluctuations in quantum phase transitions are fully quantum and driven by the Heisenberg uncertainty relation. Both classical and quantum critical points are governed by a diverging correlation length, although quantum systems possess additional correlations that do not have a classical counterpart: this is the entanglement phenomenon. Recently, a new line of exciting research points to the connection between the entanglement of a many-particle system and the appearance of quantum phase transitions [60, 66, 118, 119]. For a class of one-dimensional magnetic systems, the entanglement shows scaling behavior in the vicinity of the transition point [60]. Deeper understanding of quantum phase transitions and entanglement might be of great relevance to quantum information and computation.

Acknowledgments

I would like to thank my collaborators, Dr. Jiaxiang Wang and Hefeng Wang, for their contributions in calculating the entanglement for quantum dot systems. Also, I thank Dr. Omar Osenda, Zhen Huang, and Gehad Sadiq for their contributions to the studies of entanglement of formation and dynamics of one-dimensional magnetic systems with defects.

I also acknowledge the financial support of The National Science Foundation, the US–Israel Binational Science Foundation, and the Purdue Research Foundation.

References

1. P. O. Löwdin, *Adv. Chem. Phys.* **II**, 207 (1959).
2. E. Clementi and G. Corongiu, in *Methods and Techniques in Computational Chemistry*, METECC-95, STEF, Cagliari, 1995.
3. W. Kutzelnigg, G. Del Re, and G. Berthier, *Phys. Rev.* **172**, 49 (1968).
4. N. L. Guevara, R. P. Sagar, and R. O. Esquivel, *Phys. Rev. A* **67**, 012507 (2003).
5. P. Ziesche, O. Gunnarsson, W. John, and H. Beck, *Phys. Rev. B* **55**, 10270 (1997).
6. P. Ziesche et al., *J. Chem. Phys.* **110**, 6135 (1999).
7. P. Gersdorf, W. John, J. P. Perdew, and P. Ziesche, *Int. J. Quantum Chem.* **61**, 935 (1997).
8. Q. Shi and S. Kais, *J. Chem. Phys.* **121**, 5611 (2004).
9. S. Wilson, *Electron Correlation in Molecules*, Clarendon Press, Oxford, 1984.
10. N. H. March, *Electron Correlation in Solid State*, Imperial College Press, London, 1999.
11. C. H. Bennett and D. P. DiVincenzo, *Nature* **404**, 247 (2000).
12. C. Macchiavello, G. M. Palma, and A. Zeilinger, *Quantum Computation and Quantum Information Theory*, World Scientific, 2000.
13. M. Nielsen and I. Chuang, *Quantum Computation and Quantum Communication*, Cambridge University Press, Cambridge, 2000.
14. D. BruB, *J. Math. Phys.* **43**, 4237 (2002).
15. J. Gruska, *Quantum Computing*, McGraw-Hill, New York, 1999.
16. E. Schrödinger, *Naturwissenschaften* **23**, 807 (1935).
17. J. S. Bell, *Physics* **1**, 195 (1964).
18. A. Einstein, B. Podolsky, and N. Rosen, *Phys. Rev.* **47**, 777 (1935).
19. E. Schrödinger, *Proc. Cambridge Philos. Soc.* **31**, 555 (1935).
20. C. H. Bennett, D. P. DiVincenzo, J. A. Smolin, and W. K. Wootters, *Phys. Rev. A* **54**, 3824 (1996).
21. E. Hagley, X. Maytre, G. Nogues, C. Wunderlich, M. Brune, J. M. Raimond, and S. Haroche, *Phys. Rev. Lett.* **79**, 1(1997).
22. Q. A. Turchette, C. S. Wood, B. E. King, C. J. Myatt, D. Leibfried, W. M. Itano, C. Monroe, and D. J. Wineland, *Phys. Rev. Lett.* **81**, 3631(1998).
23. D. Bouwmeester, J.-W. Pan, M. Daniell, H. Weinfurter, and A. Zeilinger, *Phys. Rev. Lett.* **82**, 1345–1349 (1999).
24. C. Monroe, D. M. Meekhof, B. E. King, and D. J. Wineland, *Science* **272**, 1131(1996).
25. C. A. Sackett, D. Kielpinski, B. E. King, C. Langer, V. Meyer, C. J. Myatt, M. Rowe, Q. A. Turchette, W. M. Itano, D. J. Wineland, and C. Monroe, *Nature* **404**, 256–259 (2000).
26. P. Benioff, *J. Statist. Phys.* **22**, 563–591(1980); *J. Math. Phys.* **22**, 495–507(1981); *Int. J. Theor. Phys.* **21**, 177–201(1982).
27. C. H. Bennett and R. Landauer, *Sci. Am.* **253**, 48 (1985).
28. D. Deutsch, *Proc. R. Soc. A* **400**, 97 (1985); *Proc. R. Soc. A* **425**, 73 (1989).
29. R. P. Feynman, *Int. J. Theor. Phys.* **21**, 467–488(1982).
30. R. Landauer, *IBM J. Res. Dev.* **3**, 183 (1961).
31. *Proceedings of the 35th Annual Symposium on the Foundations of Computer Science*, IEEE Computer Society Press, Los Alamos, CA, 1994, p. 124; quant-ph/19508027.
32. D. Bouwmeester, K. Mattle, J.-W. Pan, H. Weinfurter, A. Zeilinger, and M. Zukowski, *Appl. Phys. B* **67**, 749 (1998).

33. D. Boyuwmester, J. W. Pan, K. Mattle, M. Eibl, H. Weinfurter, and A. Zeilinger, *Nature* **390**, 575(1997).
34. C. H. Bennett and S. J. Wiesner, *J. Phys. Rev. Lett.* **69**, 2881 (1992).
35. K. Mattle, H. Weinfurter, P. G. Kwiat, and A. Zeilinger, *Phys. Rev. Lett.* **76**, 4546 (1996).
36. B. Schumacher, *Phys. Rev. A* **51**, 2738 (1995).
37. C. H. Bennett, G. Brassard, C. Creau, R. Jozsa, A. Peres, and W. K. Wootters, *Phys. Rev. Lett.* **70**, 1895(1993).
38. M. Horodecki, *Quant. Inf. Comp.* **1**, 3 (2001).
39. P. Horodecki and R. Horodecki, *Quant. Inf. Comp.* **1**, 45 (2001).
40. W. K. Wootters, *Quant. Inf. Comp.* **1**, 27 (2001).
41. C. H. Bennett, *Phys. Rev. A* **53**, 2046 (1996).
42. W. K. Wootters, *Phys. Rev. Lett.* **80**, 2245 (1998).
43. W. K. Wootters, *Quant. Inf. Comp.* **1**, 27 (2001).
44. S. Hill and W. K. Wootters, *Phys. Rev. Lett.* **78**, 5022 (1997).
45. J. Schliemann, J. Ignacio Cirac, M. Kus, M. Lewenstein, and D. Loss, *Phys. Rev. A* **64**, 022303 (2001).
46. J. Schliemann, D. Loss, and A. H. MacDonald, e-print, cond-mat/0009083.
47. Y. S. Li, B. Zeng, X. S. Liu, and G. L. Long, *Phys. Rev. A* **64**, 054302 (2001).
48. R. Paškuskas and L. You, *Phys. Rev. A* **64**, 042310 (2001).
49. J. R. Gittings and A. J. Fisher, *Phys. Rev. A* **66**, 032305 (2002).
50. P. Zanardi, *Phys. Rev. A* **65**, 042101 (2002).
51. G. Vidal, J. I. Latorre, E. Rico, and A. Kitaev, e-print, quant-ph/0211074.
52. A. C. Doherty, P. A. Parrilo, and F. M. Spedalieri, *Phys. Rev. A* **71**, 032333 (2005).
53. B. Chong, H. Keiter, and J. Stolze, arXiv:quant-ph/0512199 (2005).
54. J. Uffink, *Phys. Rev. Lett.* **88**, 230406 (2002).
55. M. Seevinck and G. Svetlichny, *Phys. Rev. Lett.* **89**, 060401 (2002).
56. R. F. Werner, *Phys. Rev. A* **40**, 4277 (1989).
57. Z. Huang and S. Kais, *Chem. Phys. Lett.* **413**, 1 (2005).
58. C. Herring and M. Flicker, *Phys. Rev.* **134**, A362 (1964).
59. O. Osenda, Z. Huang, and S. Kais, *Phys. Rev. A* **67**, 062321 (2003).
60. A. Osterloh, L. Amico, G. Falci, and R. Fazio, *Nature* **416**, 608 (2002).
61. E. Lieb, T. Schultz, and D. Mattis, *Ann. Phys.* **60**, 407 (1961).
62. Z. Huang, O. Osenda, and S. Kais, *Phys. Lett. A* **322**, 137 (2004).
63. D. Aharonov, *Phys. Rev. A* **62**, 062311 (2000).
64. M. C. Arnesen, S. Bose, and V. Vedral, *Phys. Rev. Lett.* **87**, 017901 (2001).
65. D. Gunlycke, V. M. Kendon, and V. Vedral, *Phys. Rev. A* **64**, 042302 (2001).
66. T. J. Osborne and M. A. Nielsen, *Phys. Rev. A* **66**, 032110 (2002).
67. X. Wang, H. Fu, and A. I. Solomon, *J. Phys. A* **34**, 11307 (2001).
68. X. Wang, *Phys. Rev. A* **66**, 044395 (2002).
69. P. W. Anderson, *Science* **235**, 1196 (1987).
70. K. Onizuka et al., *J. Phys. Soc. Japan* **69**, 1016 (2000).
71. P. Jordan and E. P. Wigner, *Z. Phys.* **47**, 631 (1928).

72. E. Fradkin, *Phys. Rev. Lett.* **63**, 322 (1989).
73. A. Lopez, A. G. Rojo, and E. Fradkin, *Phys. Rev. B* **49**, 15139 (1994).
74. Y. R. Wang, *Phys. Rev. B* **43**, 3786 (1991); **45**, 12604 (1992); **45**, 12608 (1992); K. Yang, L. K. Warman, and S. M. Girvin, *Phys. Rev. Lett.* **70**, 2641 (1993).
75. O. Derzhko, *J. Phys. Studies (L'viv)* **5**, 49 (2001).
76. J. Hubbard, *Proc. R. Soc. London A* **276**, 238 (1963).
77. F. H. L. Essler, H. Frahm, F. Gohmann, A. Klumper, and V. E. Korepin, *The One-Dimensional Hubbard Model*, Cambridge University Press, Cambridge, 2005.
78. P. Zanardi, *Phys. Rev. A* **65**, 042101 (2002).
79. J. Wang and S. Kais, *Phys. Rev. A* **70**, 022301 (2004).
80. S. Gu, S. Deng, Y. Li, and H. Lin, *Phys. Rev. Lett.* **93**, 086402 (2004).
81. H. Wang and S. Kais, *Chem. Phys. Lett.* x,xx (2006).
82. H. Wang and S. Kais, *Int. J. Quantum Info.* (submitted).
83. J. Wang and S. Kais, *Int. J. Quantum Info.* **1**, 375 (2003).
84. S. Sachdev, *Quantum Phase Transitions*, Cambridge University Press, Cambridge, 1999.
85. T. J. Osborne and M. A. Nielsen, *Phys. Rev. A* **66**, 032110 (2002); e-print, quant-ph/0109024.
86. S. R. White, *Phys. Rev. Lett.* **69**, 2863 (1992).
87. G. Vidal, quant-ph/0301063, 2003; quant-ph/0310089, 2003. J. I. Latorre, E. Rico, and G. Vidal, quant-ph/0304098, 2003.
88. D. Loss and D. P. DiVincenzo, *Phys. Rev. A* **57**, 120 (1998).
89. G. Burkard, D. Loss, and D. P. DiVincenzo, *Phys. Rev. B* **59**, 2070 (1999).
90. X. Hu and S. Das Sarma, *Phys. Rev. A* **61**, 062301-1 (2000).
91. *Real-Space Renormalization*, Topics in Current Physics (T. W. Burkhardt and J. M. J. van Leeuwen, eds., Springer-Verlag, New York 1982).
92. J. X. Wang, S. Kais, and R. D. Levine, *Int. J. Mol. Sci.* **3**, 4 (2002).
93. J. X. Wang and S. Kais, *Phys. Rev. B* **66**, 081101(R) (2002).
94. J. X. Wang, S. Kais, F. Remacle, and R. D. Levine, *J. Chem. Phys. B* **106**, 12847(2002).
95. F. Remacle and R. D. Levine, *CHEMPHYSICHEM* **2**, 20 (2001).
96. M. J. Frisch et al., *Gaussian 98, Revision A.11.3*, Gaussian, Inc., Pittsburgh, PA, 1998.
97. V. A. Rassolov, M. A. Ratner, and J. A. Pople, *J. Chem. Phys.* **112**, 4014 (2000).
98. Z. Huang and S. Kais, *Int. J. Quant. Inf.* **3**, 483 (2005).
99. Z. Huang and S. Kais, *Phys. Rev. A* **73**, 022339 (2006).
100. For a review, see W. H. Zurek, *Phys. Today* **44**, 36 (1991).
101. D. Bacon, J. Kempe, D. A. Lidar, and K. B. Whaley, *Phys. Rev. Lett.* **85**, 1758 (2000).
102. N. Shevni, R. de Sousa, and K. B. Whaley, *Phys. Rev. B* **71**, 224411 (2005).
103. R. de Sousa and S. Das Sarma, *Phys. Rev. B* **68**, 115322 (2003).
104. Z. Huang, G. Sadiek, and S. Kais, *J. Chem. Phys.* x,x (2006).
105. P. Hohenberg and W. Kohn, *Phys. Rev.* **136**, B864 (1964).
106. W. Kohn and L. J. Sham, *Phys. Rev.* **140**, A1133 (1965).
107. L. A. Wu, M. S. Sarandy, D. A. Lidar, and L. J. Sham, arXiv:quant-ph/0512031 (2005).
108. A. K. Rajagopal and R. W. Rendell, arXiv:quant-ph/0512102 (2005).
109. D. R. Herschbach, J. Avery, and O. Goscinski, *Dimensional Scaling in Chemical Physics*, Kluwer, Dordrecht, 1993.

110. S. Kais and P. Serra, *Adv. Chem. Phys.* **125**, 1 (2003).
111. A. A. Svidzinsky, M. O. Scully, and D. R. Herschbach, *Phys. Rev. Lett.* **95**, 080401 (2005).
112. D. A. Mazziotti, *Phys. Rev. Lett.* **93**, 213001 (2004).
113. D. A. Mazziotti, *J. Chem. Phys.* **121**, 10957 (2004).
114. D. A. Mazziotti and R. M. Erdahl, *Phys. Rev. A* **63**, 042113 (2001).
115. E. R. Davidson, *Reduced Density Matrices in Quantum Chemistry*, Academic Press, New York, 1976.
116. H. Nakatsuji, in *Many-Electron Densities and Reduced Density Matrices* (J. Cioslowski, ed.) Kluwer, Academic, New York, 2000.
117. S. L. Sondhi, S. M. Girvin, J. P. Carini, and D. Shahar, *Rev. Mod. Phys.* **69**, 315 (1997).
118. D. Larsson and H. Johanneson, *Phys. Rev. Lett.* **95**, 196406 (2005).
119. L. A. Wu, M. S. Sarandy, and D. A. Lidar, *Phys. Rev. Lett.* **93**, 250404 (2004).